Pramana – J. Phys. (2021) 95:45
https://doi.org/10.1007/s12043-020-02065-x

Modulational instability and dynamics of discrete rational soliton and mixed interaction solutions for a higher-order nonlinear self-dual network equation

CUI-LIAN YUAN, XIAO-YONG WEN*, HAO-TIAN WANG and JUAN-JUAN WU

School of Applied Science, Beijing Information Science and Technology University, Beijing 100192, China
*Corresponding author. E-mail: xiaoyongwen@163.com

MS received 2 June 2020; revised 10 October 2020; accepted 27 October 2020

Abstract. In this paper, the higher-order nonlinear self-dual network equation is investigated. Firstly, an integrable lattice hierarchy associated with this equation is constructed from a discrete matrix spectral problem without the denominator. Secondly, the condition of modulational instability for this equation is given. Thirdly, the infinitely many conservation laws are constructed on the basis of its new Lax representation. Finally, the discrete generalised $(m, N-m)$-fold Darboux transformation (DT) with non-zero constant as seed solution is used to derive new rational soliton (RS) and mixed interaction solutions. As an application, RS solutions can be obtained by the discrete generalised $(1, N-1)$-fold DT (i.e., generalised $(m, N-m)$-fold DT with $m = 1$), and mixed interaction solutions of the usual sech-type soliton (US) and RS can be derived by the discrete generalised $(2, N-2)$-fold DT (i.e., generalised $(m, N-m)$-fold DT with $m = 2$). We also perform the numerical simulations for such soliton solutions to explore their dynamical behaviours. Results given in this paper may have some prospective applications for understanding the propagation of electrical signals.

Keywords. Higher-order nonlinear self-dual network equation; discrete generalised $(m, N-m)$-fold Darboux transformation; rational soliton solutions; mixed interaction solutions; numerical simulation.

PACS Nos 02.30.Ik; 05.45.Yv; 02.60.Cb; 04.20.Jb

1. Introduction

Nonlinear lattice equations (NLEs), which are obtained by discretising the spatial variables of the nonlinear partial differential equations (NPDEs) [1–3], can describe many physical phenomena such as nonlinear optics, plasma, physics, population dynamics, electric field, magnetic fluid, etc. [4–13]. A typical example is that nonlinear self-dual network equation can describe the propagation of electrical signals in a nonlinear, lumped, self-dual ladder-type network or nonlinear LC self-dual circuits, as shown in figure 1, in which I_n and V_n are the voltage and current in the nth capacitance and inductance respectively [11–13]. Searching for explicit exact solutions, especially soliton solutions of the NLEs, is of great significance as they can be used for depicting and explaining such nonlinear phenomena. Recently, rogue wave, which is a new type of rational solutions of some NPDEs [3], has been applied in some discrete NLEs [14,15]. It is still a very meaningful research work to explore rational solutions of NLEs, which might be helpful for understanding the corresponding phenomena in the fields of nonlinear science. Some methods to construct explicit exact solutions of NLEs have been developed such as the Hirota technique [16,17], the inverse scattering transformation [18], the algebra-geometric method [19], the N-fold Darboux transformation (DT) [20–24], etc. Among them, the N-fold DT based on Lax pair is a powerful approach to obtain multisoliton solutions without complex iterative process. Very recently, a generalised $(m, N-m)$-fold DT method has been proposed [23–27] and can be taken as a generalisation of the N-fold DT. Compared with the N-fold DT which can give usual sech-type soliton (US) solutions, the generalised $(m, N-m)$-fold DT not only expresses US solutions but also gives some rational soliton (RS) solutions and mixed interaction solutions between/among RS and US.

In the present paper, we shall apply the generalised $(m, N-m)$-fold DT method to the integrable NLEs.

Published online: 08 March 2021

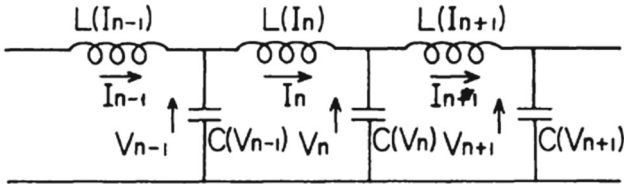

Figure 1. A ladder-type nonlinear LC circuit (see ref. [12]).

As an example, we shall focus on the following higher-order nonlinear self-dual network equation [28]:

$$\begin{cases} I_{n,t} = (I_n^2+\sigma)[I_n V_n^2 - I_n V_{n-1}^2 - I_{n-1}V_{n-1}^2 \\ \quad + I_{n+1}V_n^2 + \sigma(I_{n+1}-I_{n-1})], \\ V_{n,t} = (V_n^2+\sigma)[V_n I_{n+1}^2 + V_{n+1}I_{n+1}^2 - V_n I_n^2 \\ \quad - V_{n-1}I_n^2 + \sigma(V_{n+1}-V_{n-1})], \end{cases} \tag{1}$$

where $\sigma = \pm 1$, $I_n = I(n,t)$ and $V_n = V(n,t)$ are functions of discrete variable n and time variable t, $I_{n,t} = \mathrm{d}I_n/\mathrm{d}t$, $V_{n,t} = \mathrm{d}V_n/\mathrm{d}t$. In fact, from the physical meaning of I_n and V_n in the self-dual network equation, we can easily know that the discrete variable n is a real integer. In ref. [28], a discrete Ablowitz–Ladik hierarchy with four potentials covering eq. (1) has been given, and the symplectic map and Hamiltonian structures have been studied by means of the nonlinearisation of Lax pairs related to this integrable hierarchy including eq. (1). To be clear, eq. (1) and nonlinear self-dual network equation belong to the same hierarchy. Equation (1) is the second member in this hierarchy, and so we call eq. (1) the higher-order nonlinear self-dual network equation. Compared with nonlinear self-dual network equation, eq. (1) possesses eight more higher-order nonlinear terms in each equation which might own new properties. We know that nonlinear self-dual network equation can describe the physical phenomenon in a ladder-type electric circuit, and the two nonlinearities in nonlinear self-dual network equation denote the current-dependent inductance and the voltage-dependent capacitance respectively [11–13]. So it is noteworthy that eq. (1) contains more nonlinear terms, which may help us to better describe the propagation of electrical signals by such new nonlinear effects. Comparing with the classical nonlinear self-dual network equation in refs [11–13], eq. (1) might describe electrical signals' propagation more accurately, and physicists and engineers may design a more complicated electronic circuit diagram by using eq. (1). Yuan *et al* [29] have studied the elastic interaction of N-soliton solutions of eq. (1) via the asymptotic analysis and N-fold DT. However, as far as we know, the modulational instability (MI), infinite conservation laws, the discrete generalised $(m, N-m)$-fold DT, discrete RS solutions and mixed interaction solutions of RS and US and their dynamical behaviours of eq. (1) have not been considered before.

Therefore, in this paper, we shall further investigate eq. (1) using the generalised $(m, N-m)$-fold DT technique. The rest of this paper is organised as follows: In §2, we shall construct an integrable lattice hierarchy associated with eq. (1). In §3, we investigate the MI in the framework of eq. (1) with constants as seed solutions. In §4, infinite conservation laws of eq. (1) will be given. In §5, a discrete version of the generalised $(m, N-m)$-fold DT for eq. (1) will be constructed, and the higher-order RS and mixed interaction solutions are exhibited from the seed solutions as $I_n = a, V_n = 0$ via the resulting DT. Meanwhile, we shall discuss their dynamical behaviours and propagation characteristics via numerical simulations. Finally, we give some conclusions and discussions.

2. An integrable lattice hierarchy associated with eq. (1)

In this section, we shall construct an integrable lattice hierarchy associated with eq. (1). It is noted that the Lax pair of eq. (1) has been given in ref. [28], but it is difficult to construct the discrete generalised $(m, N-m)$-fold DT of eq. (1) because there is a denominator in its Lax pair. To construct the discrete generalised $(m, N-m)$-fold DT, we must construct a new Lax pair of eq. (1) without the denominator in its Lax pair. For this reason, we consider the following discrete matrix spectral problem:

$$E\varphi_n = M_n\varphi_n, \quad M_n = \begin{pmatrix} I_n V_n + \lambda & -\sigma I_n + \dfrac{V_n}{\lambda} \\ -\sigma\lambda V_n + I_n & \dfrac{1}{\lambda} + I_n V_n \end{pmatrix}, \tag{2}$$

where $\varphi_n = (\phi_{1,n}, \phi_{2,n})^T$ is a basic solution of eq. (2) (T denotes the transpose of a vector), λ is the spectral parameter, the discrete variable n is a real integer and the shift operator E is defined by $Ef(n,t) = f(n+1,t) \equiv f_{n+1}$, $E^{-1}f(n,t) = f(n-1,t) \equiv f_{n-1}$. To obtain an integrable lattice hierarchy associated with eq. (1), we solve the following discrete zero-curvature equation:

$$M_{n,t_m} = (EN_n^{(m)})M_n - M_n N_n^{(m)}. \tag{3}$$

Taking

$$N_n^{(m)} = \begin{pmatrix} A_n & B_n \\ C_n & D_n \end{pmatrix} = \begin{pmatrix} \sum\limits_{j=-m}^{m} A_n^{(j)}\lambda^j & \sum\limits_{j=-m}^{m-1} B_n^{(j)}\lambda^j \\ -\sigma\sum\limits_{j=-m}^{m-1} B_n^{(j)}\lambda^{-j} & \sum\limits_{j=-m}^{m} A_n^{(j)}\lambda^{-j} \end{pmatrix}$$

into eq. (3) and collecting the power coefficients of λ's various levels leads to the following recursion relations:

$$
\begin{aligned}
&\lambda^{m+1}: \quad A_{n+1}^{(m)} - A_n^{(m)} = 0,\\
&\lambda^{j}(1 \le j \le m):\\
&I_n V_n A_{n+1}^{(j)} + A_{n+1}^{(j-1)} + I_n B_{n+1}^{(j)} - \sigma V_n B_{n+1}^{(j-1)}\\
&\quad -I_n V_n A_n^{(j)} - A_n^{(j-1)} - I_n B_n^{(-j)} + \sigma V_n B_n^{(-j-1)} = 0,\\
&\sigma I_n A_n^{(-j)} - \sigma I_n A_{n+1}^{(j)} - I_n V_n B_n^{(j)} + I_n V_n B_{n+1}^{(j)}\\
&\quad -V_n A_n^{(-j-1)} + V_n A_{n+1}^{(j+1)} + B_{n+1}^{(j+1)} - B_n^{(j-1)} = 0,\\
&\lambda^{0}: \; I_n V_n A_{n+1}^{(0)} + A_{n+1}^{(-1)} + I_n B_{n+1}^{(0)} - \sigma V_n B_{n+1}^{(-1)}\\
&\quad -I_n V_n A_n^{(0)} - A_n^{(-1)} - I_n B_n^{(0)} + \sigma V_n B_n^{(-1)} = I_{n,t} V_n\\
&+I_n V_{n,t}, -I_n A_n^{(0)} + I_n A_{n+1}^{(0)} + \sigma I_n V_n B_n^{(0)}\\
&\quad -\sigma I_n V_n B_{n+1}^{(0)} + \sigma V_n A_n^{(-1)} - \sigma V_n A_{n+1}^{(1)}\\
&\quad -\sigma B_{n+1}^{(1)} + \sigma B_n^{(-1)} = I_{n,t},\\
&\lambda^{-1}: \; I_n A_n^{(1)} - \sigma I_n A_{n+1}^{(-1)} - I_n V_n B_n^{(-1)}\\
&\quad +I_n V_n B_{n+1}^{(-1)} - V_n A_n^{(0)} + V_n A_{n+1}^{(0)} + B_{n+1}^{(0)} - B_n^{(-2)}\\
&= V_{n,t}, I_n V_n A_{n+1}^{(-1)} + A_{n+1}^{(-2)} + I_n B_{n+1}^{(-1)} - \sigma V_n B_{n+1}^{(-2)}\\
&\quad -I_n V_n A_n^{(-1)} - A_n^{(-2)} - I_n B_n^{(1)} + \sigma V_n B_n^{(0)} = 0,\\
&\lambda^{j}(-m \le j \le -2):\\
&I_n V_n A_{n+1}^{(j)} + A_{n+1}^{(j-1)} + I_n B_{n+1}^{(j)} - \sigma V_n B_{n+1}^{(j-1)}\\
&\quad -I_n V_n A_n^{(j)} - A_n^{(j-1)} - I_n B_n^{(-j)} + \sigma V_n B_n^{(-j-1)} = 0,\\
&\sigma I_n A_n^{(-j)} - \sigma I_n A_{n+1}^{(j)} - I_n V_n B_n^{(j)}\\
&\quad +I_n V_n B_{n+1}^{(j)} - V_n A_n^{(-j-1)} + V_n A_{n+1}^{(j+1)}\\
&\quad +B_{n+1}^{(j+1)} - B_n^{(j-1)} = 0,\\
&\lambda^{-m-1}: \; V_n A_{n+1}^{(-m)} + B_{n+1}^{(-m)} - V_n A_n^{(m)} = 0. \qquad (4)
\end{aligned}
$$

Now we choose $A_n^{(m)} = -A_n^{(-m)} = \frac{1}{2}$. The recursion relations determine the other $A_n^{(j)}$, $A_n^{(-j)}(-m \le j \le m+1)$ and $B_n^{(j)}$, $B_n^{(-j)}(-m-1 \le j \le m)$ uniquely, and the few coefficients are given as follows:

$$
\begin{aligned}
&B_{n+1}^{(-m)} = V_n, \quad B_n^{(m-1)} = -\sigma I_n,\\
&A_n^{(m-1)} = -I_n V_{n-1}, \quad A_n^{(-m+1)} = I_n V_{n-1},\\
&B_n^{(m-2)} = \sigma I_n^2 V_n + \sigma I_n^2 V_{n-1} + V_n,\\
&B_{n+1}^{(-m+1)} = -V_n^2 I_n - I_{n+1} V_n^2 - \sigma I_n,\\
&A_n^{(m-2)} = I_n^2 V_n V_{n-1} + I_n^2 V_{n-1}^2 + I_{n-1} I_n V_{n-1}^2\\
&\qquad + \sigma I_{n-1} I_n + \sigma V_n V_{n-1},\\
&A_n^{(-m+2)} = -I_n^2 V_n V_{n-1} - I_n^2 V_{n-1}^2\\
&\qquad - I_{n-1} I_n V_{n-1}^2 - \sigma I_{n-1} I_n - \sigma V_n V_{n-1},\\
&B_{n+1}^{(-m+2)} = I_n^2 V_n^3 + I_n^2 V_n^2 V_{n-1}\\
&\qquad + 2 I_n I_{n+1} V_n^3 + I_{n+1}^2 V_n^3\\
&\qquad + I_{n+1}^2 V_n^2 V_{n+1} + \sigma I_n^2 V_n + \sigma I_n^2 V_{n-1}\\
&\qquad + 2\sigma I_n I_{n+1} V_n + \sigma V_n^2 V_{n-1}\\
&\qquad + \sigma V_n^2 V_{n+1} + V_{n-1},\\
&B_n^{(m-3)} = -\sigma I_n^3 V_n^2 - 2\sigma I_n^3 V_n V_{n-1} - \sigma I_n^3 V_{n-1}^2\\
&\qquad - \sigma I_n^2 I_{n-1} V_{n-1}^2 - \sigma I_n^2 I_{n+1} V_n^2 - I_n^2 I_{n-1}\\
&\qquad - I_n^2 I_{n+1} - I_n V_n^2 - 2 I_n V_n V_{n-1}\\
&\qquad - I_{n+1} V_n^2 - \sigma I_{n+1},\\
&A_n^{(m-3)} = -I_n^3 V_n^2 V_{n-1} - 2 I_n^3 V_n V_{n-1}^2 - I_n^3 V_{n-1}^3\\
&\qquad - I_n^2 I_{n-1} V_n V_{n-1}^2 - 2 I_n^2 I_{n-1} V_{n-1}^3\\
&\qquad - I_n^2 I_{n+1} V_n^2 V_{n-1} - I_n I_{n-1}^2 V_{n-2} V_{n-1}^2\\
&\qquad - I_n I_{n-1}^2 V_{n-1}^3 - \sigma I_n^2 I_{n-1} V_n\\
&\qquad - 2\sigma I_n^2 I_{n-1} V_{n-1} - \sigma I_n^2 I_{n+1} V_{n-1}\\
&\qquad - \sigma I_n I_{n-1}^2 V_{n-2} - \sigma I_n I_{n-1}^2 V_{n-1}\\
&\qquad - \sigma I_n V_n^2 V_{n-1} - 2\sigma I_n V_n V_{n-1}^2\\
&\qquad - \sigma I_n V_{n-2} V_{n-1}^2 - \sigma I_{n-1} V_n V_{n-1}^2\\
&\qquad - \sigma I_{n+1} V_n^2 V_{n-1} - I_n V_{n-2} - I_{n-1} V_n\\
&\qquad - I_{n+1} V_{n-1},\\
&A_n^{(-m+3)} = I_n^3 V_n^2 V_{n-1} + 2 I_n^3 V_n V_{n-1}^2\\
&\qquad + I_n^3 V_{n-1}^3 + I_n^2 I_{n-1} V_n V_{n-1}^2 + 2 I_n^2 I_{n-1} V_{n-1}^3\\
&\qquad + I_n^2 I_{n+1} V_n^2 V_{n-1} + I_n I_{n-1}^2 V_{n-2} V_{n-1}^2\\
&\qquad + I_n I_{n-1}^2 V_{n-1}^3 + \sigma I_n^2 I_{n-1} V_n\\
&\qquad + 2\sigma I_n^2 I_{n-1} V_{n-1} + \sigma I_n^2 I_{n+1} V_{n-1}\\
&\qquad + \sigma I_n I_{n-1}^2 V_{n-2} + \sigma I_n I_{n-1}^2 V_{n-1}\\
&\qquad + \sigma I_n V_n^2 V_{n-1} + 2\sigma I_n V_n V_{n-1}^2\\
&\qquad + \sigma I_n V_{n-2} V_{n-1}^2\\
&\qquad + \sigma I_{n-1} V_n V_{n-1}^2 + \sigma I_{n+1} V_n^2 V_{n-1}\\
&\qquad + I_n V_{n-2} + I_{n-1} V_n + I_{n+1} V_{n-1}, \ldots,\\
&A_n^{(j-1)} = (E-1)^{-1}(-I_n V_n A_{n+1}^{(j)} - I_n B_{n+1}^{(j)}\\
&\qquad + \sigma V_n B_{n+1}^{(j-1)} + I_n V_n A_n^{(j)} + I_n B_n^{(-j)}\\
&\qquad - \sigma V_n B_n^{(-j-1)}) \;\; (1 \le j \le m+1),\\
&A_n^{(-j+1)} = -A_n^{(j-1)} \;\; (2 \le j \le m+1),\\
&B_n^{(j-1)} = \sigma I_n A_n^{(-j)} - \sigma I_n A_{n+1}^{(j)} - I_n V_n B_n^{(j)}\\
&\qquad + I_n V_n B_{n+1}^{(j)} - V_n A_n^{(-j-1)} + V_n A_{n+1}^{(j+1)}\\
&\qquad + B_{n+1}^{(j+1)} \;\; (1 \le j \le m),\\
&B_{n+1}^{(j+1)} = -\sigma I_n A_n^{(-j)} + \sigma I_n A_{n+1}^{(j)}
\end{aligned}
$$

$$+I_nV_nB_n^{(j)}-I_nV_nB_{n+1}^{(j)}+V_nA_n^{(-j-1)}-V_nA_{n+1}^{(j+1)}+B_n^{(j-1)}(-m-1\le j\le -2). \tag{5}$$

The discrete zero-curvature equation (3) gives rise to the following integrable lattice hierarchy:

with

$$\begin{aligned}A_n &= \frac{\lambda^2}{2}-\lambda I_nV_{n-1}+I_n^2V_nV_{n-1}\\ &\quad +I_n^2V_{n-1}^2+I_nI_{n-1}V_{n-1}^2+\sigma I_nI_{n-1}\\ &\quad +\sigma V_nV_{n-1}+I_nV_{n-1}\frac{1}{\lambda}-\frac{1}{2\lambda^2},\end{aligned}$$

$$\begin{cases} I_{n,t_m}=\sigma I_nV_nB_n^{(0)}-\sigma I_nV_nB_{n+1}^{(0)}+\sigma V_nA_n^{(-1)}-\sigma V_nA_{n+1}^{(1)}-\sigma B_{n+1}^{(1)}+\sigma B_n^{(-1)}-I_nA_n^{(0)}+I_nA_{n+1}^{(0)},\\ V_{n,t_m}=\sigma I_nA_n^{(1)}-\sigma I_nA_{n+1}^{(-1)}-I_nV_nB_n^{(-1)}+I_nV_nB_{n+1}^{(-1)}-V_nA_n^{(0)}+V_nA_{n+1}^{(0)}+B_{n+1}^{(0)}-B_n^{(-2)}. \end{cases} \tag{6}$$

When $m=1$, using recursion relations (4) with (5), system (6) reduces to the famous nonlinear self-dual network equation [11–13]:

$$\begin{cases} I_{n,t_1}=(I_n^2+\sigma)(V_{n-1}-V_n),\\ V_{n,t_1}=(V_n^2+\sigma)(I_n-I_{n+1}), \end{cases} \tag{7}$$

which is the same as that in ref. [28], and the time part of its Lax pair is given by

$$\begin{aligned}N_n^{(1)} &= \begin{pmatrix} A_n^{(1)}\lambda+A_n^{(0)}+\dfrac{A_n^{(-1)}}{\lambda} & B_n^{(0)}+\dfrac{B_n^{(-1)}}{\lambda}\\ -\sigma(B_n^{(-1)}\lambda+B_n^{(0)}) & A_n^{(-1)}\lambda+A_n^{(0)}+\dfrac{A_n^{(1)}}{\lambda}\end{pmatrix}\\ &= \begin{pmatrix} \frac{\lambda}{2}-I_nV_{n-1}-\dfrac{1}{2\lambda} & -\sigma I_n+\dfrac{V_{n-1}}{\lambda}\\ -\sigma\lambda V_{n-1}+I_n & -\dfrac{\lambda}{2}-I_nV_{n-1}+\dfrac{1}{2\lambda}\end{pmatrix}.\end{aligned} \tag{8}$$

When $m=2$, system (6) reduces to eq. (1), whose time part of the Lax pair is given by

$$\begin{aligned}B_n &= -\sigma\lambda I_n+\sigma I_n^2V_n+\sigma I_n^2V_{n-1}+V_n\\ &\quad -(\sigma I_{n-1}+I_nV_{n-1}^2+I_{n-1}V_{n-1}^2)\frac{1}{\lambda}+V_{n-1}\frac{1}{\lambda^2},\\ C_n &= -\sigma\lambda^2V_{n-1}+\lambda(\sigma I_nV_{n-1}^2+\sigma I_{n-1}V_{n-1}^2+I_{n-1})\\ &\quad -\sigma I_n^2V_n-V_n-I_n^2V_{n-1}+I_n\frac{1}{\lambda},\\ D_n &= -\frac{1}{2}\lambda^2+\lambda I_nV_{n-1}+\sigma I_{n-1}I_n\\ &\quad +\sigma V_{n-1}V_n+I_n^2V_{n-1}V_n+I_n^2V_{n-1}^2\\ &\quad +I_{n-1}I_nV_{n-1}^2-I_nV_{n-1}\frac{1}{\lambda}+\frac{1}{2\lambda^2}.\end{aligned}$$

Here we need to point out that eq. (1) has more nonlinear terms than nonlinear self-dual network equation (7), which may possess new properties. The new Lax pairs (2) and (9) do not contain the denominator different from the one in ref. [28], which is more convenient to construct its DT. Therefore in what follows, we shall further investigate eq. (1) and discuss its relevant properties.

When $m=3$, system (6) reduces to the following new third-order nonlinear self-dual network equation:

$$\begin{cases} I_{n,t_3}=(I_n^2+\sigma)[-I_n^2V_n^3-I_n^2V_n^2V_{n-1}+I_n^2V_nV_{n-1}^2+I_n^2V_{n-1}^3+2I_nI_{n-1}V_{n-1}^3-2I_nI_{n+1}V_n^3+I_{n-1}^2V_{n-2}V_{n-1}^2\\ \qquad +I_{n-1}^2V_{n-1}^3-I_{n+1}^2V_n^3-I_{n+1}^2V_n^2V_{n+1}+\sigma(2I_nI_{n-1}V_{n-1}-2I_nI_{n+1}V_n+I_{n-1}^2V_{n-2}+I_{n-1}^2V_{n-1}\\ \qquad -I_{n+1}^2V_n-I_{n+1}^2V_{n+1}-V_n^2V_{n-1}-V_n^2V_{n+1}+V_nV_{n-1}^2+V_{n-2}V_{n-1}^2)+V_{n-2}-V_{n+1}],\\ V_{n,t_3}=(V_n^2+\sigma)[I_n^3V_n^2+2I_n^3V_nV_{n-1}+I_n^3V_{n-1}^2+I_n^2I_{n-1}V_{n-1}^2+I_n^2I_{n+1}V_n^2-I_nI_{n+1}^2V_n^2-I_{n+1}^3V_n^2\\ \qquad -2I_{n+1}^3V_nV_{n+1}-I_{n+1}^3V_{n+1}^2-I_{n+1}^2I_{n+2}V_{n+1}^2+\sigma(I_n^2I_{n-1}+I_n^2I_{n+1}-I_nI_{n+1}^2+2I_nV_nV_{n-1}+I_nV_{n-1}^2\\ \qquad +I_{n-1}V_{n-1}^2-I_{n+1}^2I_{n+2}-2I_{n+1}V_nV_{n+1}-I_{n+1}V_{n+1}^2-I_{n+2}V_{n+1}^2)+I_{n-1}-I_{n+2}]. \end{cases} \tag{10}$$

$$\begin{aligned}N_n^{(2)} &= \begin{pmatrix} A_n & B_n\\ C_n & D_n\end{pmatrix}\\ &= \begin{pmatrix} \sum\limits_{j=-2}^{2}A_n^{(j)}\lambda^j & \sum\limits_{j=-2}^{1}B_n^{(j)}\lambda^j\\ -\sigma\sum\limits_{j=-2}^{1}B_n^{(j)}\lambda^{-j} & \sum\limits_{j=-2}^{2}A_n^{(j)}\lambda^{-j}\end{pmatrix},\end{aligned} \tag{9}$$

Thus, we can give a new more higher-order nonlinear self-dual network equation which includes 40 more nonlinear terms in each equation of (10) relative to the classical nonlinear self-dual network equation and eq. (1). Similarly, eq. (10) may help to design more complicated electrical circuits in LC circuits which might describe more complex physical phenomena. Accordingly, the time part of the Lax pair for (10) is as follows:

$$N_n^{(3)} = \begin{pmatrix} A_n & B_n \\ C_n & D_n \end{pmatrix} = \begin{pmatrix} \sum_{j=-3}^{3} A_n^{(j)}\lambda^j & \sum_{j=-3}^{2} B_n^{(j)}\lambda^j \\ -\sigma \sum_{j=-3}^{2} B_n^{(j)}\lambda^{-j} & \sum_{j=-3}^{3} A_n^{(j)}\lambda^{-j} \end{pmatrix} \tag{11}$$

with

$$\begin{aligned}
A_n =& (I_n^2V_nV_{n-1} + I_n^2V_{n-1}^2 + I_nI_{n-1}V_{n-1}^2 \\
&+\sigma I_nI_{n-1} + \sigma V_nV_{n-1})\lambda \\
&-(I_n^2V_nV_{n-1} + I_n^2V_{n-1}^2 + I_nI_{n-1}V_{n-1}^2 \\
&+\sigma I_nI_{n-1} + \sigma V_nV_{n-1})\frac{1}{\lambda} - I_n^3V_{n-1}^3 - V_nI_{n-1} \\
&-I_nV_{n-2} - I_{n+1}V_{n-1} - I_nI_{n-1}^2V_{n-2}V_{n-1}^2 \\
&-I_{n+1}I_n^2V_{n-1}V_n^2 - I_n^2V_nI_{n-1}V_{n-1}^2 - 2I_n^3V_nV_{n-1}^2 \\
&-I_nV_{n-1}\lambda^2 - 2I_n^2I_{n-1}V_{n-1}^3 + I_nV_{n-1}\frac{1}{\lambda^2} \\
&-2\sigma I_n^2I_{n-1}V_{n-1} - 2\sigma I_nV_nV_{n-1}^2 \\
&-\sigma I_{n+1}V_{n-1}V_n^2 - \sigma I_{n+1}I_n^2V_{n-1} - \sigma I_nV_{n-2}V_{n-1}^2 \\
&-\sigma I_nV_n^2V_{n-1} - \sigma I_n^2V_nI_{n-1} - \sigma I_nI_{n-1}^2V_{n-1} \\
&-\sigma I_nI_{n-1}^2V_{n-2} - \sigma V_nI_{n-1}V_{n-1}^2 - I_nI_{n-1}^2V_{n-1}^3 \\
&-I_n^3V_n^2V_{n-1} - \frac{1}{2\lambda^3} + \frac{1}{2}\lambda^3, \\
B_n =& -\sigma I_n\lambda^2 + (\sigma I_n^2V_n + \sigma I_n^2V_{n-1} + V_n)\lambda \\
&-\sigma I_n^3V_n^2 - 2\sigma I_n^3V_nV_{n-1} - \sigma I_n^3V_{n-1}^2 \\
&-\sigma I_n^2I_{n-1}V_{n-1}^2 - \sigma I_n^2I_{n+1}V_n^2 - I_n^2I_{n-1} \\
&-I_n^2I_{n+1} - I_nV_n^2 - 2I_nV_nV_{n-1} - I_{n+1}V_n^2 \\
&-\sigma I_{n+1} + (I_n^2V_nV_{n-1}^2 + I_n^2V_{n-1}^3 \\
&+2I_nI_{n-1}V_{n-1}^3 + I_{n-1}^2V_{n-2}V_{n-1}^2 + I_{n-1}^2V_{n-1}^3 \\
&+2\sigma I_nI_{n-1}V_{n-1} + \sigma I_{n-1}^2V_{n-2} + \sigma I_{n-1}^2V_{n-1} \\
&+\sigma V_nV_{n-1}^2 + \sigma V_{n-2}V_{n-1}^2 + V_{n-2})\frac{1}{\lambda} \\
&+(-I_nV_{n-1}^2 - I_{n-1}V_{n-1}^2 - \sigma I_{n-1})\frac{1}{\lambda^2} + V_{n-1}\frac{1}{\lambda^3}, \\
C_n =& I_n\frac{1}{\lambda^2} - (I_n^2V_n + I_n^2V_{n-1} + \sigma V_n)\frac{1}{\lambda} + I_n^3V_n^2 \\
&+2I_n^3V_nV_{n-1} + I_n^3V_{n-1}^2 + I_n^2I_{n-1}V_{n-1}^2 \\
&+I_n^2I_{n+1}V_n^2 + \sigma I_n^2I_{n-1} + \sigma I_n^2I_{n+1} + \sigma I_nV_n^2 \\
&+2\sigma I_nV_nV_{n-1} + \sigma I_{n+1}V_n^2 + I_{n+1} - (\sigma I_n^2V_nV_{n-1}^2 \\
&+\sigma I_n^2V_{n-1}^3 + 2\sigma I_nI_{n-1}V_{n-1}^3 + \sigma I_{n-1}^2V_{n-2}V_{n-1}^2 \\
&+\sigma I_{n-1}^2V_{n-1}^3 + 2I_nI_{n-1}V_{n-1} + I_{n-1}^2V_{n-2} \\
&+I_{n-1}^2V_{n-1} + V_nV_{n-1}^2 + V_{n-2}V_{n-1}^2 + \sigma V_{n-2})\lambda \\
&+(\sigma I_nV_{n-1}^2 + \sigma I_{n-1}V_{n-1}^2 + I_{n-1})\lambda^2 - \sigma V_{n-1}\lambda^3,
\end{aligned}$$

$$\begin{aligned}
D_n =& -2\sigma I_n^2I_{n-1}V_{n-1} - 2\sigma I_nV_nV_{n-1}^2 - I_nV_{n-1}\frac{1}{\lambda^2} \\
&-2I_n^3V_nV_{n-1}^2 - 2I_n^2I_{n-1}V_{n-1}^3 - \sigma I_{n+1}V_{n-1}V_n^2 \\
&-\sigma I_{n+1}I_n^2V_{n-1} - \sigma I_nV_n^2V_{n-1} \\
&-\sigma V_nI_{n-1}V_{n-1}^2 - \sigma I_nI_{n-1}^2V_{n-2} - \sigma I_nI_{n-1}^2V_{n-1} \\
&-\sigma I_nV_{n-2}V_{n-1}^2 - I_nI_{n-1}^2V_{n-1}^3 - I_n^3V_n^2V_{n-1} \\
&-\sigma I_n^2V_nI_{n-1} - (I_n^2V_nV_{n-1} + I_n^2V_{n-1}^2 + I_nI_{n-1}V_{n-1}^2 \\
&+\sigma I_nI_{n-1} + \sigma V_nV_{n-1})\lambda + (I_n^2V_nV_{n-1} + I_n^2V_{n-1}^2 \\
&+I_nI_{n-1}V_{n-1}^2 + \sigma I_nI_{n-1} + \sigma V_nV_{n-1})\frac{1}{\lambda} - I_n^3V_{n-1}^3 \\
&-V_nI_{n-1} - I_nV_{n-2} - I_{n+1}V_{n-1} \\
&+\frac{1}{2\lambda^3} - I_nI_{n-1}^2V_{n-2}V_{n-1}^2 - I_{n+1}I_n^2V_{n-1}V_n^2 \\
&-I_n^2V_nI_{n-1}V_{n-1}^2 + I_nV_{n-1}\lambda^2 - \frac{1}{2}\lambda^3.
\end{aligned}$$

3. Modulational instability

The modulational instability (MI) may be the main cause of localised waves. In this section, we investigate the MI for eq. (1) starting from seed solutions $I_0 = a$, $V_0 = b$, adding small amplitude to its seed solution as $I_n = I_0 + \epsilon F_n(t)$ and $V_n = V_0 + \epsilon G_n(t)$, where $F_n = F_n(t)$ and $G_n = G_n(t)$ are the perturbation functions of n and t, ϵ is an infinitesimal amplitude of the perturbation. Substituting I_n and V_n into eq. (1) yields the real-valued linearised perturbation coupled system

$$\begin{aligned}
&F_{n,t} + 4ab(a^2+\sigma)(G_{n-1} - G_n) \\
&\quad +(a^2+\sigma)(b^2+\sigma)(F_{n-1} - F_{n+1}) = 0, \\
&G_{n,t} + 4ab(b^2+\sigma)(F_n - F_{n+1}) \\
&\quad -(a^2+\sigma)(b^2+\sigma)(G_{n+1} - G_{n-1}) = 0.
\end{aligned} \tag{12}$$

We take $F_n = P\mathrm{e}^{gt+ikn}$ and $G_n = Q\mathrm{e}^{gt+ikn}$, where P and Q are real constant amplitudes of the perturbation eigenmode, g denotes the frequency and k is the arbitrary real wave number of the small perturbations. Similar to ref. [27], substituting F_n and G_n into eq. (12), it can produce one system of coupled linear equations for P and Q. The system has non-trivial solutions only when g, k satisfy a dispersion relation, namely

$$\begin{aligned}
g =& 8\sqrt{-a^2b^2(a^2+\sigma)(b^2+\sigma)\sin^2\left(\frac{k}{2}\right)} \\
&+2i(a^2+\sigma)(b^2+\sigma)\sin k.
\end{aligned} \tag{13}$$

We define the MI gain $G = |\Re(g)|$, where $\Re$ represents the real part. Figure 2 displays the MI gain map

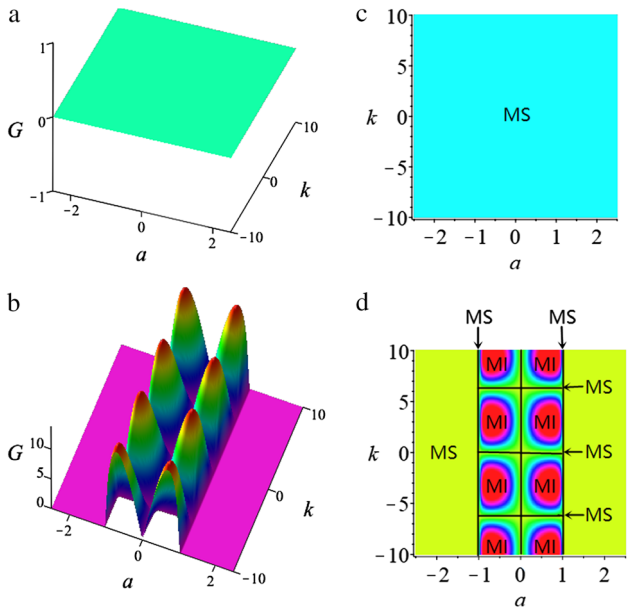

Figure 2. (**a**), (**c**) MI gain G vs. k and a when $b = 0, \sigma = 1$; (**b**), (**d**) MI gain G vs. k and a when $b = 2, \sigma = -1$. MI and MS denote modulational instability and modulational stability.

vs. k and a. When $\sigma = 1$, for all possible values of b, the expression g in eq. (13) is pure imaginary and the MI gain G is equal to zero, which implies that the MI does not occur. Figures 2a and 2c show one region which is modulation stability (MS) when $b = 0$ and $\sigma = 1$. When $\sigma = -1$, the expression g in eq. (13) has real parts and the MI gain G is non-zero, which implies that there are two distinctive regions including MI and MS, as shown in figures 2b and 2d, which show two distinctive regions including MI and MS when $b = 2$ and $\sigma = -1$. In MI regions, small perturbations are unstable and can be amplified exponentially, while in the MS regions they are stable and do not grow up.

According to ref. [30], for the sake of discussion, we set $A = -a^2b^2(a^2 + \sigma)(b^2 + \sigma)\sin^2(k/2)$. Then two cases will be discussed as follows:

- For $\sigma = 1$, for all possible parameter values, $A \leq 0$, that is to say, the MI gain $G = 0$, which implies that the MI does not occur, and the whole region is stable. In this case, the US and RS excitation can occur in the MS region which are confirmed in the subsequent RS solutions and numerical simulation of this paper.
- For $\sigma = -1$, if $k \neq 2m\pi$, $m \in Z$, $|a| > 1$, $|b| < 1$ or $|a| < 1$, $|b| > 1$, then $A > 0$, which implies that the MI occurs. For the other cases, we have $A \leq 0$, which implies that the MI does not occur. Especially, for $k = 2m\pi$ or $a = \pm 1$, then $A = 0$, the regions in these lines are MS.

4. Conservation laws of eq. (1)

Existence of conservation laws plays an important role in proving their integrability for integrable system [31]. In this part, we shall derive the infinitely many conservation laws for eq. (1). Some physical properties such as energy, momentum and Hamiltonian conservation laws can be described by the first three conservation laws.

From Lax pairs (2) and (9), we can get

$$\varphi_{1,n+1} = (\lambda + I_n V_n)\varphi_{1,n} + \left(\frac{V_n}{\lambda} - \sigma I_n\right)\varphi_{2,n},$$
$$\varphi_{2,n+1} = (I_n - \sigma\lambda V_n)\varphi_{1,n} + \left(\frac{1}{\lambda} + I_n V_n\right)\varphi_{2,n}. \quad (14)$$

Setting $\theta_n = \varphi_{2,n}/\varphi_{1,n}$, we obtain

$$\frac{\varphi_{1,n+1}}{\varphi_{1,n}} = \lambda + I_n V_n + \left(\frac{V_n}{\lambda} - \sigma I_n\right)\theta_n,$$
$$\frac{\varphi_{2,n+1}}{\varphi_{2,n}} = \frac{I_n - \sigma\lambda V_n}{\theta_n} + \frac{1}{\lambda} + I_n V_n, \quad (15)$$

from which we have

$$\left(\frac{V_n}{\lambda} - \sigma I_n\right)\theta_n\theta_{n+1} + (\lambda + I_n V_n)\theta_{n+1} - \left(\frac{1}{\lambda} + I_n V_n\right)\theta_n - I_n + \sigma\lambda V_n = 0. \quad (16)$$

Suppose that

$$\theta_n = \sum_{j=0}^{\infty} \frac{\theta_n^{(j)}}{\lambda^j}, \quad (17)$$

and substitution of (17) into (16) leads to the following recursion relations:

$$\begin{aligned}
\theta_n^{(0)} &= -\sigma V_{n-1},\\
\theta_n^{(1)} &= I_{n-1}(\sigma V_{n-1}^2 + 1),\\
\theta_n^{(2)} &= -(\sigma V_{n-1}^2 + 1)(I_{n-1}^2 V_{n-2} + I_{n-1}^2 V_{n-1} + \sigma V_{n-2}),\\
\theta_n^{(3)} &= (\sigma V_{n-1}^2 + 1)(I_{n-1}^3(V_{n-2} + V_{n-1})^2 + I_{n-2}I_{n-1}^2(V_{n-2}^2 + \sigma) + \sigma I_{n-1}V_{n-2}(V_{n-2} + 2V_{n-1}) + I_{n-2}(\sigma V_{n-2}^2 + 1)),\\
\theta_n^{(4)} &= -(\sigma V_{n-1}^2 + 1)(I_{n-1}^4(V_{n-2} + V_{n-1})^3 + 2I_{n-2}I_{n-1}^3(V_{n-2}^2 + \sigma)(V_{n-2} + V_{n-1}) + I_{n-1}^2(I_{n-2}^2(V_{n-2}^2 + \sigma)(V_{n-3} + V_{n-2}) + \sigma V_{n-2}^3 + \sigma(V_{n-3} + 4V_{n-1})V_{n-2}^2 + 3\sigma V_{n-2}V_{n-1}^2 + V_{n-3}) + 2I_{n-1}I_{n-2}(\sigma V_{n-2}^2 + 1)(V_{n-2} + V_{n-1})
\end{aligned} \quad (18)$$

$$+I_{n-2}^2(\sigma V_{n-2}^2+1)(V_{n-3}+V_{n-2})$$
$$+(V_{n-3}+V_{n-1})V_{n-2}^2+\sigma V_{n-3}).$$

Equations (9) and (15) lead to

$$\left[\ln\left(\lambda+I_nV_n+\left(\frac{V_n}{\lambda}-\sigma I_n\right)\theta_n\right)\right]_t = (E-1)(A_n+B_n\theta_n), \tag{19}$$

where

$$\begin{aligned}
A_n &= \frac{\lambda^2}{2}-\lambda I_nV_{n-1}+I_n^2V_nV_{n-1}\\
&\quad +I_n^2V_{n-1}^2+I_nI_{n-1}V_{n-1}^2+\sigma I_nI_{n-1}\\
&\quad +\sigma V_nV_{n-1}+I_nV_{n-1}\frac{1}{\lambda}-\frac{1}{2\lambda^2},\\
B_n &= -\sigma\lambda I_n+\sigma I_n^2V_n+\sigma I_n^2V_{n-1}\\
&\quad +V_n-(\sigma I_{n-1}+I_nV_{n-1}^2+I_{n-1}V_{n-1}^2)\frac{1}{\lambda}\\
&\quad +V_{n-1}\frac{1}{\lambda^2}.
\end{aligned}$$

Substituting (19) into (19) and equating the same powers of λ in (19) generate the infinitely many conservation laws for eq. (1), and the first three conservation laws are listed as follows:

$$(T_k)_t = (E-1)(X_k), \quad (k=1,2,3) \tag{20}$$

with

$$\begin{aligned}
T_1 &= I_n(V_n+V_{n-1}),\\
X_1 &= (V_{n-1}^2+\sigma)(I_nI_{n-1}^2(V_{n-2}+V_{n-1})\\
&\quad +I_{n-1}(I_n^2+\sigma)(V_n+V_{n-1})+\sigma I_n(V_{n-2}+V_{n-1})),\\
T_2 &= -\frac{1}{2}I_n^2(V_n+V_{n-1})^2-I_{n-1}I_n(V_{n-1}^2+\sigma)\\
&\quad -\sigma V_nV_{n-1},\\
X_2 &= -I_n^2(V_n+V_{n-1})(V_{n-1}^2+\sigma)\\
&\quad \times(I_{n-1}^2(V_{n-2}+V_{n-1})+\sigma V_{n-2})-I_n(I_{n-1}^2+\sigma)\\
&\quad \times(V_{n-1}^2+\sigma)(I_{n-1}(V_{n-2}+V_{n-1})^2\\
&\quad +I_{n-2}(V_{n-2}^2+\sigma))-I_{n-1}^2(\sigma V_{n-1}^2+1)\\
&\quad \times(V_nV_{n-2}+V_nV_{n-1}+V_{n-1}^2+\sigma)\\
&\quad -(V_nV_{n-2}+\sigma)V_{n-1}^2-\sigma V_nV_{n-2}-\frac{1}{2},\\
T_3 &= \frac{1}{3}I_n^3(V_n+V_{n-1})^3+I_{n-1}I_n^2(V_{n-1}^2+\sigma)\\
&\quad \times(V_n+V_{n-1})+I_n(I_{n-1}^2(V_{n-1}^2+\sigma)(V_{n-2}+V_{n-1})\\
&\quad +\sigma(V_n+V_{n-2})V_{n-1}^2+\sigma V_n^2V_{n-1}+V_{n-2})\\
&\quad +I_{n-1}V_n(\sigma V_{n-1}^2+1),\\
X_3 &= (V_{n-1}^2+\sigma)(I_nI_{n-1}^4(V_{n-2}+V_{n-1})^3\\
&\quad +I_{n-1}^3(V_{n-2}+V_{n-1})(I_n^2(V_{n-2}+V_{n-1})(V_n+V_{n-1})\\
&\quad +I_{n-2}I_n(2V_{n-2}^2+2\sigma)+\sigma V_nV_{n-2}\\
&\quad +\sigma V_nV_{n-1}+\sigma V_{n-1}^2+1)\\
&\quad +I_{n-1}^2(I_{n-2}I_n^2(V_{n-2}^2+\sigma)(V_n+V_{n-1})\\
&\quad +I_n(I_{n-2}^2(V_{n-2}^2+\sigma)(V_{n-3}+V_{n-2})+\sigma V_{n-2}^3\\
&\quad +\sigma(V_{n-3}+4V_{n-1})V_{n-2}^2+4\sigma V_{n-2}V_{n-1}^2\\
&\quad +\sigma V_{n-1}^3+V_{n-3})+I_{n-2}V_n(\sigma V_{n-2}^2+1))\\
&\quad +I_{n-1}(\sigma I_n^2V_{n-2}(V_{n-2}+2V_{n-1})(V_n+V_{n-1})\\
&\quad +2I_nI_{n-2}(\sigma V_{n-2}^2+1)(V_{n-2}+V_{n-1})+V_nV_{n-2}^2\\
&\quad +(2V_nV_{n-1}+V_{n-1}^2+\sigma)V_{n-2}+\sigma V_{n-1})\\
&\quad +I_{n-2}I_n^2(\sigma V_{n-2}^2+1)(V_n+V_{n-1})\\
&\quad +I_n(I_{n-2}^2(\sigma V_{n-2}^2+1)(V_{n-3}+V_{n-2})\\
&\quad +(V_{n-3}+V_{n-1})V_{n-2}^2+V_{n-2}V_{n-1}^2+\sigma V_{n-3})\\
&\quad +I_{n-2}V_n(V_{n-2}^2+\sigma)),
\end{aligned}$$

where T_k and X_k are the conserved densities and associated fluxes, respectively. The first three conservation laws represent the energy, momentum and Hamiltonian laws, respectively.

5. Discrete generalised $(m, N-m)$-fold DT

In this section, we shall construct the generalised $(m, N-m)$-fold DT of eq. (1) based on the basis of Lax pair (2) and (9). First, we assume that $\varphi_n(\lambda_i) = (\phi_n(\lambda_i), \psi_n(\lambda_i))^T$ $(i=1,2,\ldots,m)$ are m distinct solutions of (2) and (9) for m spectral parameters $\lambda_i (i=1,2,\ldots,m)$ and the initial solutions I_n, V_n of eq. (1). We introduce the following special gauge transformation:

$$\tilde{\varphi}_n = T_n\varphi_n = \begin{pmatrix} \lambda^N+\sum\limits_{j=0}^{N-1}a_n^{(j)}\lambda^j & \sum\limits_{j=0}^{N-1}b_n^{(j)}\lambda^j \\ -\sigma\sum\limits_{j=0}^{N-1}b_n^{(j)}\lambda^{N-j} & 1+\sum\limits_{j=0}^{N-1}a_n^{(j)}\lambda^{N-j} \end{pmatrix}\varphi_n, \tag{21}$$

which ensures that $\tilde{\varphi}_n$ satisfies $E\tilde{\varphi}_n = \tilde{M}_n\tilde{\varphi}_n$ and $\tilde{\varphi}_{n,t} = \widetilde{N_n^{(2)}}\tilde{\varphi}_n$. From the knowledge of DT, we know that M_n and $N_n^{(2)}$ have the same forms with $\tilde{M}_n$ and $\widetilde{N_n^{(2)}}$ under transformations $\tilde{M}_n = T_{n+1}M_nT_n^{-1}$ and $\widetilde{N_n^{(2)}} = (T_{n,t}+T_nN_n^{(2)})T_n^{-1}$, except replacing the old potentials I_n, V_n with new ones $\tilde{I}_n$, $\tilde{V}_n$. It should be noted that N is a positive integer in (21), and $a_n^{(j)}$ and $b_n^{(j)}$, which are

the functions of variables n and t, can be determined by the following linear algebraic system with $2N$ equations ($N = m + \sum_{i=1}^{n} M_i, i = 1, 2, \ldots, m$):

$$\begin{cases} T_n^{(0)}(\lambda_i)\varphi_n^{(0)}(\lambda_i) = 0, \\ T_n^{(0)}(\lambda_i)\varphi_n^{(1)}(\lambda_i) + T_n^{(1)}(\lambda_i)\varphi_n^{(0)}(\lambda_i) = 0, \\ T_n^{(0)}(\lambda_i)\varphi_n^{(2)}(\lambda_i) + T_n^{(1)}(\lambda_i)\varphi_n^{(1)}(\lambda_i) \\ + T_n^{(2)}(\lambda_i)\varphi_n^{(0)}(\lambda_i) = 0, \\ \cdots\cdots, \\ \sum_{j=0}^{M_i} T_n^{(j)}(\lambda_i)\varphi_n^{(M_i-j)}(\lambda_i) = 0, \end{cases} \tag{22}$$

$$\tilde{I}_n = \frac{I_n + \sigma b_n^{(N-1)}}{a_n^{(0)}}, \quad \tilde{V}_n = b_{n+1}^{(0)} + V_n a_{n+1}^{(0)} \tag{23}$$

with

$$a_n^{(0)} = \frac{\Delta a_n^{(0)}}{\Delta_N^{\varepsilon(m)}}, \quad b_n^{(0)} = \frac{\Delta b_n^{(0)}}{\Delta_N^{\varepsilon(m)}}, \quad b_n^{(N-1)} = \frac{\Delta b_n^{(N-1)}}{\Delta_N^{\varepsilon(m)}},$$
$$\Delta_N^{\varepsilon(m)} = \det([\Delta^{(1)}, \Delta^{(2)}, \ldots, \Delta^{(m)}]^T), \tag{24}$$

where $\Delta^{(i)} = (\Delta_{j,s}^{(i)})_{2(M_i+1)\times 2N}$, *in which* $\Delta_{j,s}^{(i)} (1 \le j \le 2M_i + 2, 1 \le s \le N, i = 1, 2, \ldots, m)$ *are given by the following formulae*:

$$\Delta_{j,s}^{(i)} = \begin{cases} \sum_{k=0}^{j-1} C_{N-s}^k \lambda_i^{N-s-k} \phi^{(j-1-k)} & \text{for} \quad 1 \le j \le M_i + 1, \quad 1 \le s \le N, \\ \sum_{k=0}^{j-1} C_{2N-s}^k \lambda_i^{2N-s-k} \psi^{(j-1-k)} & \text{for} \quad 1 \le j \le M_i + 1, \quad N+1 \le s \le 2N, \\ \sum_{k=0}^{j-(N+1)} C_s^k \lambda_i^{s-k} \psi^{(j-1-N-k)} & \text{for} \quad M_i + 2 \le j \le 2(M_i+1), \quad 1 \le s \le N, \\ -\sigma \sum_{k=0}^{j-(N+1)} C_{s-N}^k \lambda_i^{s-N-k} \phi^{(j-N-1-k)} & \text{for} \quad M_i + 2 \le j \le 2(M_i+1), \quad N+1 \le s \le 2N, \end{cases}$$

where $T_n^{(i)}$ is derived by

$$T_n(\lambda_i + \varepsilon) = T_n^{(0)} + T_n^{(1)}\varepsilon + \cdots + T_n^{(M_i)}\varepsilon^{M_i},$$

while $\varphi_n^{(k)}$ is determined by

$$\varphi_n(\lambda_i + \varepsilon) = \varphi_n^{(0)}(\lambda_i) + \varphi_n^{(0)}(\lambda_i)\varepsilon^2 + \varphi_n^{(0)}(\lambda_i)\varepsilon^4 + \cdots$$

and

$$\varphi_n^{(k)}(\lambda_i) = \frac{1}{k!}\frac{\partial^k}{\partial \lambda_i^k}\varphi_n(\lambda_i).$$

According to the above analysis and discrete version of generalised $(m, N-m)$-fold DT in refs [24–27], we can verify that eq. (1) admits the following discrete generalised $(m, N-m)$-fold DT:

Theorem 1. *Let* $\varphi_i(\lambda_i) = (\phi_i(\lambda_i), \psi_i(\lambda_i))^T$ *be column vector solutions with distinct spectral parameters* $\lambda_i (i = 1, 2, \ldots, m)$ *of* (2) *and* (9) *and* (I_n, V_n) *is the same seed solutions of eq.* (1)*, as considered above, then the generalised perturbation* $(m, N-m)$*-fold DT for eq.* (1) *is given by*

$$b_j = \begin{cases} -\sum_{k=0}^{j-1} C_N^k \lambda_i^{N-k} \phi^{(j-1-k)} & \text{for} \quad 1 \le j \le M_i + 1, \\ -\psi^{(j-N-1)} & \text{for} \quad M_i + 2 \le j \le 2(M_i+1). \end{cases}$$

and $\Delta a_n^{(0)}$, $\Delta b_n^{(0)}$ *and* $\Delta b_n^{(N-1)}$ *are given by the determinant* $\Delta_N^{\varepsilon(m)}$ *replacing its* N*th,* $(2N)$*th and* $(N+1)$*th columns by the column vector* $b = (b_j)_{2N\times 1}$ *with*

Here $a_{n+1}^{(0)}$ *and* $b_{n+1}^{(1)}$ *are obtained from* $a_n^{(0)}$ *and* $b_n^{(1)}$ *by replacing* n *with* $n+1$.

Remark 1. Here m denotes the number of the distinct spectral parameters, N denotes the order number and $N-m$ denotes the sum of the order number of the highest derivative of the Darboux matrix T_n or the vector eigenfunction φ_n. Notice that when $m = N$, the N-fold DT is a special case of the discrete generalised $(N, 0)$-fold DT, which can be used to construct multisoliton solutions in ref. [29]. When $m = 1$, Theorem 1 can reduce to the discrete generalised $(1, N-1)$-fold DT, which is used to get high-order RS solutions of eq. (1). When $m = 2$, Theorem 1 can reduce to the discrete generalised $(2, N-2)$-fold DT, which is used to obtain

mixed interaction solutions of US and RS, and it should be noted that these new solutions are not singular. For other cases, new DTs can also be derived, which we are not discussing here. Next, we shall use the discrete generalised $(1, N-1)$-fold and $(2, N-2)$-fold DTs to construct RS solutions and mixed interaction solutions of US and RS for eq. (1) from the non-zero seed solutions.

5.1 *Discrete generalised* $(1, N-1)$*-fold DT*

In what follows, we produce rational solutions in terms of determinants introduced above for eq. (1) with $\sigma = 1$ by means of the discrete generalised $(1, N-1)$-fold DT. For the case $\sigma = -1$, the process is similar and will not be discussed due to its solutions possessing singularity. Substitution of $I_n = a$, $V_n = 0$ into (2) and (9) yields the following basic solution:

$$\varphi_n(\lambda) = \begin{pmatrix} C_1\tau_1^n e^{\rho_1 t+\theta(\varepsilon)} + C_2\tau_2^n e^{\rho_2 t} \\ C_1\dfrac{\lambda-\tau_1}{a}\tau_1^n e^{\rho_1 t+\theta(\varepsilon)} + C_2\dfrac{\lambda-\tau_2}{a}\tau_2^n e^{\rho_2 t} \end{pmatrix} \tag{25}$$

with

$$\tau_1 = \frac{1}{2\lambda}(\lambda^2+1+\sqrt{-(2a\lambda+\lambda^2-1)(2a\lambda-\lambda^2+1)}),$$

$$\tau_2 = \frac{1}{2\lambda}(\lambda^2+1-\sqrt{-(2a\lambda+\lambda^2-1)(2a\lambda-\lambda^2+1)}),$$

$$\rho_1 = \frac{1}{2\lambda^2}(2a^2\lambda^2+(\lambda^2+1) \times\sqrt{-(2a\lambda+\lambda^2-1)(2a\lambda-\lambda^2+1)}),$$

$$\rho_2 = \frac{1}{2\lambda^2}(2a^2\lambda^2-(\lambda^2+1) \times\sqrt{-(2a\lambda+\lambda^2-1)(2a\lambda-\lambda^2+1)}),$$

$$\theta(\varepsilon) = \sqrt{-(2a\lambda+\lambda^2-1)(2a\lambda-\lambda^2+1)}\sum_{k=1}^{N} d_k\varepsilon^{2k},$$

where C_1, C_2 are arbitrary constants, $d_k (k = 1, 2, \ldots, N)$ are free real coefficients and ε is an artificially introduced small parameter.

Next, we fix the spectral parameter in eq. (35) as $\lambda = \lambda_1 + \varepsilon^2$ with $\lambda_1 = a + \sqrt{a^2+1}$, and expand vector function φ_n in eq. (35) into the Taylor series around $\varepsilon = 0$, explicitly calculating the coefficients of the expansion in φ_n. In particular, choosing $C_1 = -C_2 = 1/\varepsilon$, $a = 3/4$, (i.e., $\lambda_1 = 2$), we have

$$\varphi(\varepsilon^2) = \sum_{j=0}^{\infty}\varphi_1^{(j)}\varepsilon^{2j} = \varphi^{(0)} + \varphi^{(1)}\varepsilon^2 + \varphi^{(2)}\varepsilon^4 + \varphi^{(3)}\varepsilon^6 + \cdots, \tag{26}$$

where

$$\varphi_n^{(0)} = \begin{pmatrix}\phi^{(0)}\\ \psi^{(0)}\end{pmatrix} = \left(\frac{5}{4}\right)^n\frac{\sqrt{15}}{60}e^{(9/16)t}\begin{pmatrix}3\xi\\ 3\xi-40\end{pmatrix}, \tag{27}$$

$$\varphi_n^{(1)} = \begin{pmatrix}\phi^{(1)}\\ \psi^{(1)}\end{pmatrix} = \left(\frac{5}{4}\right)^n\frac{\sqrt{15}}{38400}e^{(9/16)t}\begin{pmatrix}3\xi^3+112\xi+19200t\\ 3\xi^3-120\xi^2+1712\xi+19200t-\dfrac{12160}{3}\end{pmatrix}, \tag{28}$$

$$\varphi_n^{(2)} = \begin{pmatrix}\phi^{(2)}\\ \psi^{(2)}\end{pmatrix} = \left(\frac{5}{4}\right)^n\frac{\sqrt{15}}{2211840000}e^{(9/16)t}\begin{pmatrix}81\xi^5+30240\xi^3+5184000\xi^2t-5496576\xi+326246400t\\ 81\xi^5-5400\xi^4+174240\xi^3+5184000\xi^2t-138240000\xi t\\ -1900800\xi^2+1247846400t-9336576\xi+43059200\end{pmatrix}, \tag{29}$$

where $\xi = 25t + 8n$ and the remaining $\varphi_n^{(j)}$ $(j \geq 3)$ are omitted here.

According to the discrete generalised $(1, N-1)$-fold DT in Theorem 1, we shall discuss three cases: $N = 1, 2$ and 3.

5.1.1 *First-order RS solutions and dynamical behaviours.*

For $N = 1$, according to Theorem 1, based on the discrete generalised $(1, 0)$-fold DT, we can give the first-order RS solutions of eq. (1) as

$$\tilde{I}_n = \frac{a+b_n^{(0)}}{a_n^{(0)}}, \quad \tilde{V}_n = b_{n+1}^{(0)}, \tag{30}$$

where

$$a_n^{(0)} = \frac{\Delta a_n^{(0)}}{\Delta_1^{\varepsilon}}, \quad b_n^{(0)} = \frac{\Delta b_n^{(0)}}{\Delta_1^{\varepsilon}}$$

with

$$\Delta_1^{\varepsilon} = \begin{vmatrix}\phi^{(0)} & \psi^{(0)}\\ \lambda_1\psi^{(0)} & -\lambda_1\phi^{(0)}\end{vmatrix},$$

$$\Delta a_n^{(0)} = \begin{vmatrix}-\lambda_1\phi^{(0)} & \psi^{(0)}\\ -\psi^{(0)} & -\lambda_1\phi^{(0)}\end{vmatrix},$$

$$\Delta b_n^{(0)} = \begin{vmatrix}\phi^{(0)} & -\lambda_1\phi^{(0)}\\ \lambda_1\psi^{(0)} & -\psi^{(0)}\end{vmatrix},$$

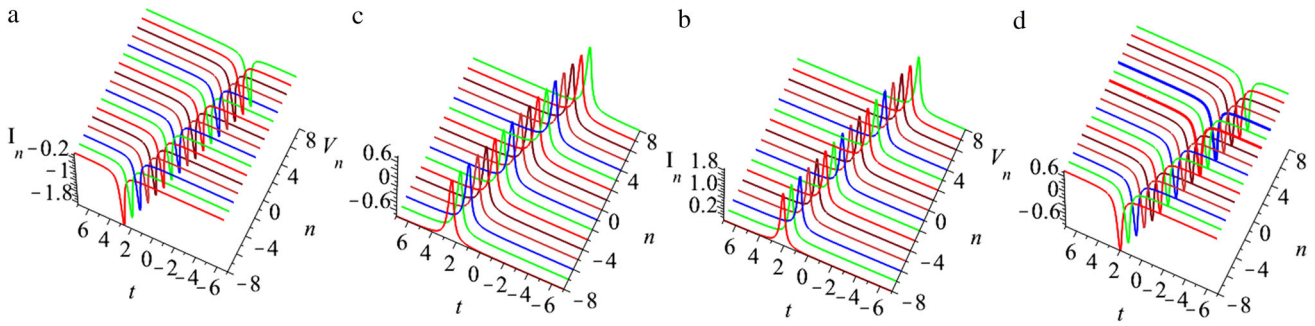

Figure 3. Evolution plots of the first-order RS solutions $\tilde{I}_n$ and $\tilde{V}_n$ with different parameters (**a**), (**c**) $a = 3/4, \lambda_1 = 2$; (**b**), (**d**) $a = -3/4, \lambda_1 = 1/2$.

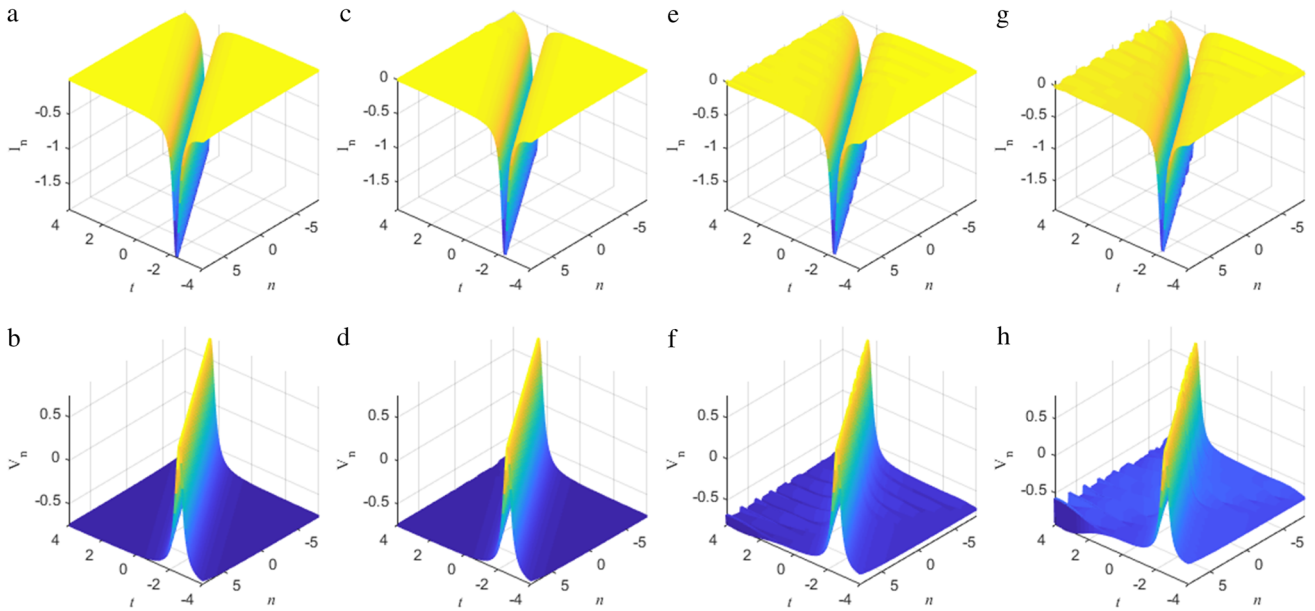

Figure 4. Numerical simulations of the first-order RS solutions $\tilde{I}_n$ and $\tilde{V}_n$ given by eq. (31) with the same parameters as in figures 3a and 3c. (**a**), (**b**) exact solution; (**c**), (**d**) unperturbed situation; (**e**), (**f**) perturbed by the initial 2% noise; (**g**), (**h**) perturbed by the initial 5% noise.

while $b_{n+1}^{(0)}$ are obtained from $b_n^{(0)}$ by replacing n with $n+1$. Then

$$\tilde{I}_n = -\frac{480}{9(\xi - \frac{8}{3})^2 + 256},$$
$$\tilde{V}_n = -\frac{3}{4} + \frac{600}{9(\xi + \frac{4}{3})^2 + 400} \tag{31}$$

which have no singularity for all real n and t. It is important to point out that we have obtained the non-singular rational rogue wave solutions of discrete NLEs [25,27], while in refs [24,26], we have obtained the singular rational solutions of discrete NLEs, and for NPDEs, the non-singular RS solutions of mKdV equation have been given in ref. [23]. However, here we shall give the non-singular discrete rational solutions of eq. (1), whose structures are similar to the usual sech-type soliton and different forms of rogue wave solutions. We call these non-singular solutions (31) the discrete RS solutions. Figure 3 displays the first-order dark and bright RS structures of solutions (31). From figures 3a and 3c we can see that the valley of the dark RS solution I_n and the peak of the bright RS solution V_n are localised along the lines $3\xi - 8 = 0$ and $3\xi + 4 = 0$ respectively. Along the line $3\xi - 8 = 0$, I_n reaches the minimum which is $-15/8$, while along the line $3\xi + 4 = 0$, V_n reaches the maximum which is $3/4$. In addition, if $a > 0$, then I_n is a dark RS, while V_n is a bright RS. When $a < 0$, the situation is just opposite (see figures 3b and 3d).

To study whether the above-obtained RS solutions are stable during the propagation process, we perform the numerical simulations to explore the dynamics of some of the above-mentioned RSs of eq. (1) by using

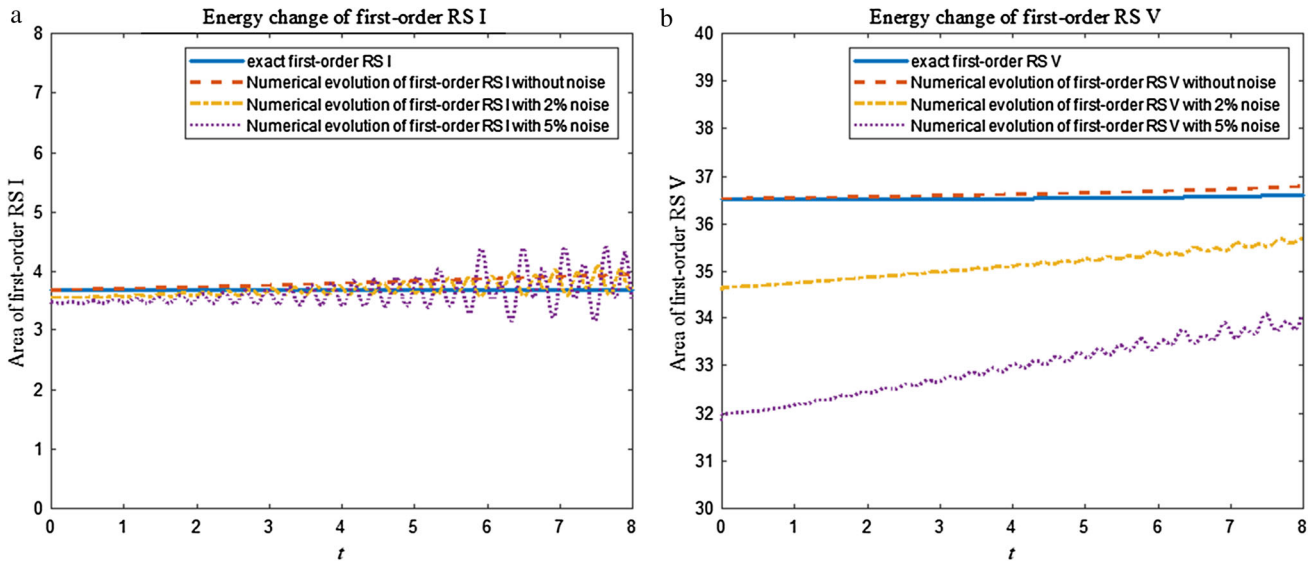

Figure 5. Energy changes of numerical results of the first-order RS solutions in figure 4.

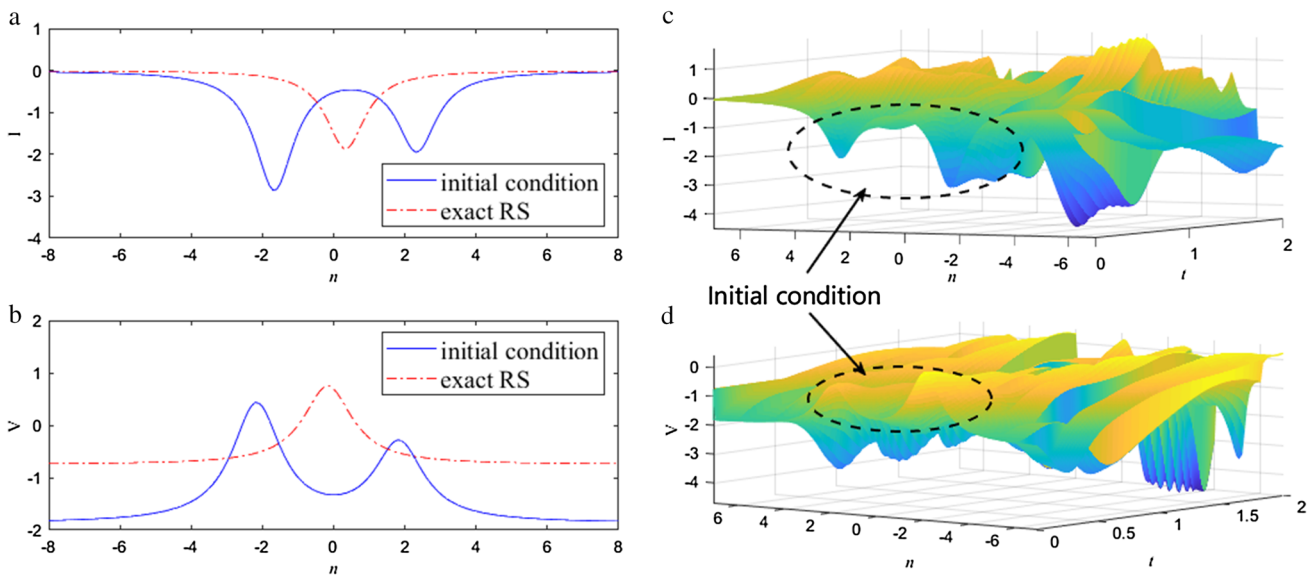

Figure 6. (**a**), (**b**) Exact first-order RS solutions $\tilde{I}_n$, $\tilde{V}_n$ and initial solution $1.5I_{n\to n-2,t=0} + I_{n\to n+2,t=0}$, $1.5V_{n\to n-2,t=0} + V_{n\to n+2,t=0}$; (**c**), (**d**) the interaction of exact first-order RS solutions $\tilde{I}_n$, $\tilde{V}_n$ and another first-order RS solutions $1.5I_{n\to n-2,t=0}$, $1.5V_{n\to n-2,t=0}$.

the finite difference method [32]. Figures 4a–4d respectively show the numerical results of the exact first-order RS solutions and the unperturbed exact first-order RS solutions as an initial condition from $t = -4$, and we find that the time evolutions of the RS solutions without noises is very close to the exact RS solutions. Figures 4e–4h display the numerical results of the perturbed situation by multiplying the analytical first-order RS solutions by 2% and 5% noises as the initial condition, respectively. These results show that the 2% or 5% noise has little effect on the evolutions of the first-order RS solutions. Moveover, figures 5a and 5b show energy changes of I_n and V_n, from which we can see more clearly that first-order RS solution of I_n can remain as the stable evolutions for a longer period with 2% and 5% noises, while solution V_n has obvious energy change and remains as the unstable evolutions with noises.

In addition, we also use $I_n = 1.5I_{n\to n-2,t=0} + I_{n\to n+2,t=0}$ and $V_n = 1.5V_{n\to n-2,t=0} + V_{n\to n+2,t=0}$ as initial conditions to model the wave propagation. The

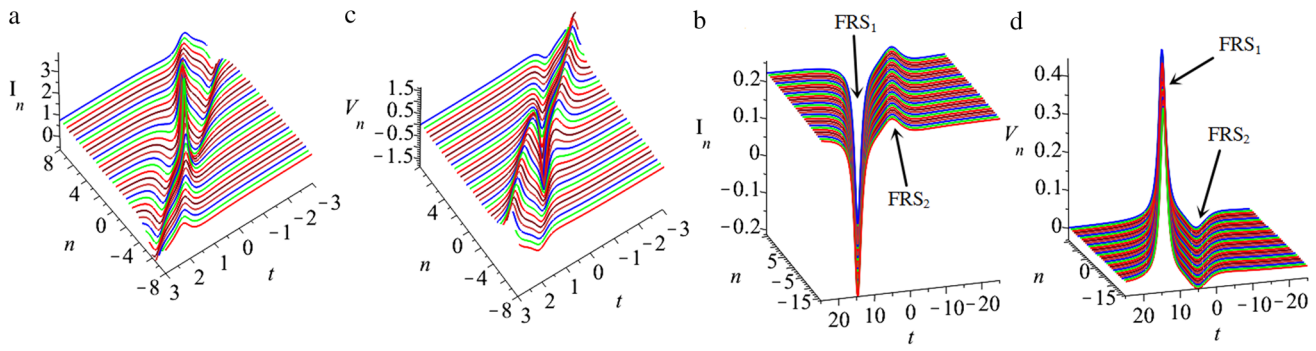

Figure 7. Evolution plots of the second-order RS solutions $\tilde{I}_n$ and $\tilde{V}_n$ with different parameters (**a**), (**c**) $a = 3/4, \lambda_1 = 2, d_1 = 0$; (**b**), (**d**) $a = 9/40, \lambda_1 = 5/4, d_1 = 200$. The phrases FRS_1 and FRS_2 stand for two parallel first-order RS solutions which are derived from the second-order RS solution.

results exhibit non-elastic collision phenomenon of two first-order RSs (see figure 6).

5.1.2 *Second-order RS solutions and dynamical behaviours.* According to Theorem 1, for $N = 2$, based on the discrete generalised (1, 1)-fold DT, the second-order RS solutions of eq. (1) are given by

$$\tilde{I}_n = \frac{a + b_n^{(1)}}{a_n^{(0)}}, \quad \tilde{V}_n = b_{n+1}^{(0)}, \tag{32}$$

where

$$a_n^{(0)} = \frac{\Delta a_n^{(0)}}{\Delta_2^{\varepsilon}}, \quad b_n^{(0)} = \frac{\Delta b_n^{(0)}}{\Delta_2^{\varepsilon}}$$

and

$$b_n^{(1)} = \frac{\Delta b_n^{(1)}}{\Delta_2^{\varepsilon}}$$

with

$$\Delta_2^{\varepsilon} = \begin{vmatrix} \lambda_1\phi^{(0)} & \phi^{(0)} & \lambda_1\psi^{(0)} & \psi^{(0)} \\ \lambda_1\phi^{(1)} + \phi^{(0)} & \phi^{(1)} & \lambda_1\psi^{(1)} + \psi^{(0)} & \psi^{(1)} \\ \lambda_1\psi^{(0)} & \lambda_1^2\psi^{(0)} & -\lambda_1\phi^{(0)} & -\lambda_1^2\phi^{(0)} \\ \lambda_1\psi^{(1)} + \psi^{(0)} & \lambda_1^2\psi^{(1)} + 2\lambda_1\psi^{(0)} & -\lambda_1\phi^{(1)} - \phi^{(0)} & -\lambda_1^2\phi^{(1)} - 2\lambda_1\phi^{(0)} \end{vmatrix},$$

in which $\Delta a_n^{(0)}$, $\Delta b_n^{(0)}$ and $\Delta b_n^{(1)}$ are given by determinant Δ_2^{ε} by replacing its second, fourth and third columns by the column vector $(-\lambda_1^2\phi^{(0)}, -\lambda_1^2\phi^{(1)} - 2\lambda_1\phi^{(0)}, -\psi^{(0)}, -\psi^{(1)})^T$, while $b_{n+1}^{(0)}$ are obtained from $b_n^{(1)}$ by replacing n with $n + 1$. Then by simplifying the above expressions we have

$$\tilde{I}_n = \frac{F_1}{G_1}, \quad \tilde{V}_n = \frac{F_2}{G_2}, \tag{33}$$

where

$$\begin{aligned}
F_1 &= 243\xi^6 - 3888\xi^5 - 14256\xi^4 \\
&\quad +(-1555200t + 152064)\xi^3 \\
&\quad +(12441600t - 2239488)\xi^2 \\
&\quad +(-215654400t - 11059200)\xi \\
&\quad +2488320000t^2 + 1105920000t \\
&\quad +491520000, \\
G_1 &= 324\xi^6 - 5184\xi^5 + 67392\xi^4 \\
&\quad +(-2073600t - 718848)\xi^3 \\
&\quad +(16588800t + 18210816)\xi^2 \\
&\quad +(265420800t - 49152000)\xi \\
&\quad +3317760000t^2 + 163840000, \\
F_2 &= 12960(\xi + 8)^4 - 345600(\xi + 8)^3 \\
&\quad +6082560(\xi + 8)^2 \\
&\quad +(82944000t - 40550400)(\xi + 8) \\
&\quad -552960000t, \\
G_2 &= 81(\xi + 8)^6 - 3240(\xi + 8)^5 \\
&\quad +58320(\xi+8)^4+(-518400t - 656640)(\xi+8)^3 \\
&\quad +(10368000t + 7455744)(\xi + 8)^2 \\
&\quad +(-16588800t - 49152000)(\xi + 8) \\
&\quad +829440000t^2 + 163840000.
\end{aligned}$$

For $d_1 = 0$, the second-order RS solutions (33) exhibit strong interaction (see figures 7a and 7c), while for $d_1 = 200$, the second-order RS solutions (33) are split into the nearly parallel interactions of one dark RS and one bright RS solutions (see figures 7b and 7d).

Next, we studied the dynamical behaviour of the second-order RS solutions via numerical simulations. Figures 8a–8d exhibit the numerical results of the unperturbed exact second-order RS solutions and the unperturbed analytical second-order RS solutions, which show that the evolutions of the second-order RS solutions without a noise almost coincides with the corresponding exact RS solutions. Figures 8e–8h display the numerical results of the perturbed situation by adding 2% and 5% noises to the initial conditions. These results show that the evolutions with 2% and 5% noises have the same evolutions in comparison with the unperturbed solutions. Figures 9a–9d exhibit the numerical results of the unperturbed exact separable second-order RS solutions and the unperturbed analytical separable second-order RS solutions. Figures 9e–9h display the numerical results of the perturbed situation by adding 2% and 5% noises to the initial conditions. These above results exhibit strong stability and are also robust against small noises.

5.1.3 *Third-order RS solutions and dynamical behaviours.* Similarly, according to Theorem 1, performing the analogous calculating process for $N = 3$, the third-order RS solutions of eq. (1) can be given by

$$\tilde{I}_n = \frac{a + b_n^{(2)}}{a_n^{(0)}}, \quad \tilde{V}_n = b_{n+1}^{(0)}, \tag{34}$$

where

$$a_n^{(0)} = \frac{\Delta a_n^{(0)}}{\Delta_3^{\varepsilon}},$$

$$b_n^{(0)} = \frac{\Delta b_n^{(0)}}{\Delta_3^{\varepsilon}}$$

and

$$b_n^{(2)} = \frac{\Delta b_n^{(2)}}{\Delta_3^{\varepsilon}}$$

with

$$\Delta_3^{\varepsilon} = \begin{vmatrix} \lambda_1^2\phi^{(0)} & \lambda_1\phi^{(0)} & \phi^{(0)} & \lambda_1^2\psi^{(0)} & \lambda_1\psi^{(0)} & \psi^{(0)} \\ \Delta^{(2,1)} & \Delta^{(2,2)} & \Delta^{(2,3)} & \Delta^{(2,4)} & \Delta^{(2,5)} & \Delta^{(2,6)} \\ \Delta^{(3,1)} & \Delta^{(3,2)} & \Delta^{(3,3)} & \Delta^{(3,4)} & \Delta^{(3,5)} & \Delta^{(3,6)} \\ \lambda_1\psi^{(0)} & \lambda_1^2\psi^{(0)} & \lambda_1^3\psi^{(0)} & -\lambda_1\phi^{(0)} & -\lambda_1^2\phi^{(0)} & -\lambda_1^3\phi^{(0)} \\ \Delta^{(5,1)} & \Delta^{(5,2)} & \Delta^{(5,3)} & \Delta^{(5,4)} & \Delta^{(5,5)} & \Delta^{(5,6)} \\ \Delta^{(6,1)} & \Delta^{(6,2)} & \Delta^{(6,3)} & \Delta^{(6,4)} & \Delta^{(6,5)} & \Delta^{(6,6)} \end{vmatrix},$$

$\Delta^{(2,1)} = \lambda_1^2\phi^{(1)} + 2\lambda_1\phi^{(0)}$, $\Delta^{(2,2)} = \lambda_1\phi^{(1)} + \phi^{(0)}$, $\Delta^{(2,3)} = \phi^{(1)}$, $\Delta^{(2,4)} = \lambda_1^2\psi^{(1)} + 2\lambda_1\psi^{(0)}$, $\Delta^{(2,5)} = \lambda_1\psi^{(1)} + \psi^{(0)}$, $\Delta^{(2,6)} = \psi^{(1)}$, $\Delta^{(3,1)} = \lambda_1^2\phi^{(2)} + 2\lambda_1\phi^{(1)} + \phi^{(0)}$, $\Delta^{(3,2)} = \lambda_1\phi^{(2)} + \phi^{(1)}$, $\Delta^{(3,3)} = \phi^{(2)}$, $\Delta^{(3,4)} = \lambda_1^2\psi^{(2)} + 2\lambda_1\psi^{(1)} + \psi^{(0)}$, $\Delta^{(3,5)} = \lambda_1\psi^{(2)} + \psi_{(1)}$, $\Delta^{(3,6)} = \psi^{(2)}$, $\Delta^{(5,1)} = \lambda_1\psi^{(1)} + \psi^{(0)}$, $\Delta^{(5,2)} = \lambda_1^2\psi^{(1)} + 2\lambda_1\psi^{(0)}$, $\Delta^{(5,3)} = \lambda_1^3\psi^{(1)} + 3\lambda_1^2\psi^{(0)}$, $\Delta^{(5,4)} = -\lambda_1\phi^{(1)} - \phi^{(0)}$, $\Delta^{(5,5)} = -\lambda_1^2\phi^{(1)} - 2\lambda_1\phi^{(0)}$, $\Delta^{(5,6)} = -\lambda_1^3\phi^{(1)} - 3\lambda_1^2\phi^{(0)}$, $\Delta^{(6,1)} = \lambda_1\psi^{(2)} + \psi^{(1)}$, $\Delta^{(6,2)} = \lambda_1^2\psi^{(2)} + 2\lambda_1\psi^{(1)} + \psi^{(0)}$, $\Delta^{(6,3)} = \lambda_1^3\psi^{(2)} + 3\lambda_1^2\psi^{(1)} + 3\lambda_1\psi^{(0)}$, $\Delta^{(6,4)} = -\lambda_1\phi^{(2)} - \phi^{(1)}$, $\Delta^{(6,5)} = -\lambda_1^2\phi^{(2)} - 2\lambda_1\phi^{(1)} - \phi^{(0)}$, $\Delta^{(6,6)} = -\lambda_1^3\phi^{(2)} - 3\lambda_1^2\phi^{(1)} - 3\lambda_1\phi^{(0)}$ and $\Delta a_n^{(0)}$, $\Delta b_n^{(0)}$ and $\Delta b_n^{(2)}$ are given by determinant Δ_3^{ε} replacing its third, sixth and fourth columns by the column vector $(-\lambda_1^3\phi^{(0)}, -\lambda_1^3\phi^{(1)} - 3\lambda_1^2\phi^{(0)}, -\lambda_1^3\phi^{(2)} - 3\lambda_1^2\phi^{(1)} - 3\lambda_1\phi^{(0)}, -\psi^{(0)}, -\psi^{(1)}, -\psi^{(2)})^T$, while $a_{n+1}^{(0)}$ and $b_{n+1}^{(0)}$ are obtained from $a_n^{(0)}$ and $b_n^{(0)}$ by replacing n with $n + 1$. Solutions (34) are too complicated and therefore omitted here.

The parameters d_1, d_2 excite the third-order RS solutions to generate abundant wave structures. Next, we discuss some special structures of the third-order RS for the following four cases:

- When $d_1 = d_2 = 0, a = 3/4$, the strong interactions of the third-order RS solutions are shown in figures 10a and 10e.
- When $d_1 = 100, d_2 = 0, a = 9/40$, the weak interactions of the third-order RS solutions I_n and V_n are shown in figures 10b and 10f, from which we can see that the third-order RS is split into three first-order parallel RSs with two first-order bright RSs and one first-order dark RS.
- When $d_2 = 800, d_1 = 0, a = 9/40$, the weak interactions of the third-order RS solutions I_n and V_n are shown in figures 10c and 10g. This shows a similar situation to figures 10b and 10f, while they have different space structures.
- When $d_1 = 100, d_2 = 400, a = 9/40$, the weak interactions of the third-order RS solutions I_n and V_n are shown in figures 10d and 10h, which shows a similar situation to figures 10b, 10f and 10c, 10g. However, they have different space distribution.

Moreover, the dynamics of the third-order RS solutions given by eq. (34) are considered. Figures 11 and 12 respectively show the numerical results of third-order strong and weak RS solutions, which also display that

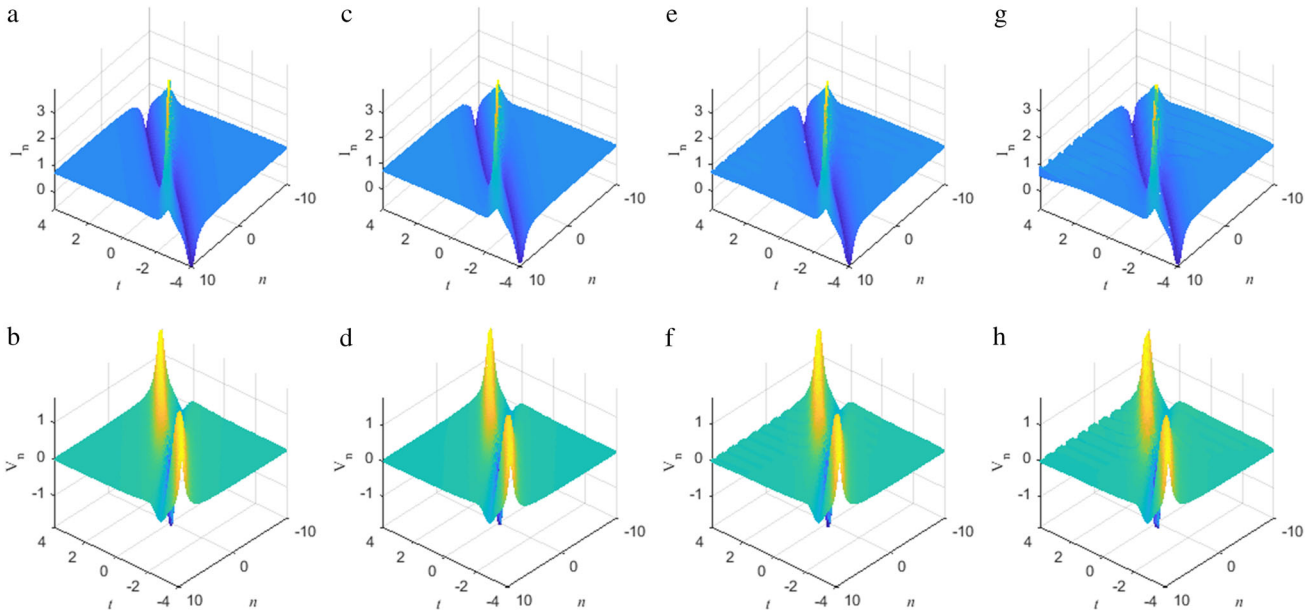

Figure 8. Numerical simulations of the second-order RS solutions $\tilde{I}_n$ and $\tilde{V}_n$ given by eq. (33) with the same parameters as in figures 7a and 7c. (**a**) and (**b**) exact solution; (**c**) and (**d**) unperturbed situation; (**e**) and (**f**) perturbed by the initial 2% noise; (**g**) and (**h**) perturbed by the initial 5% noise.

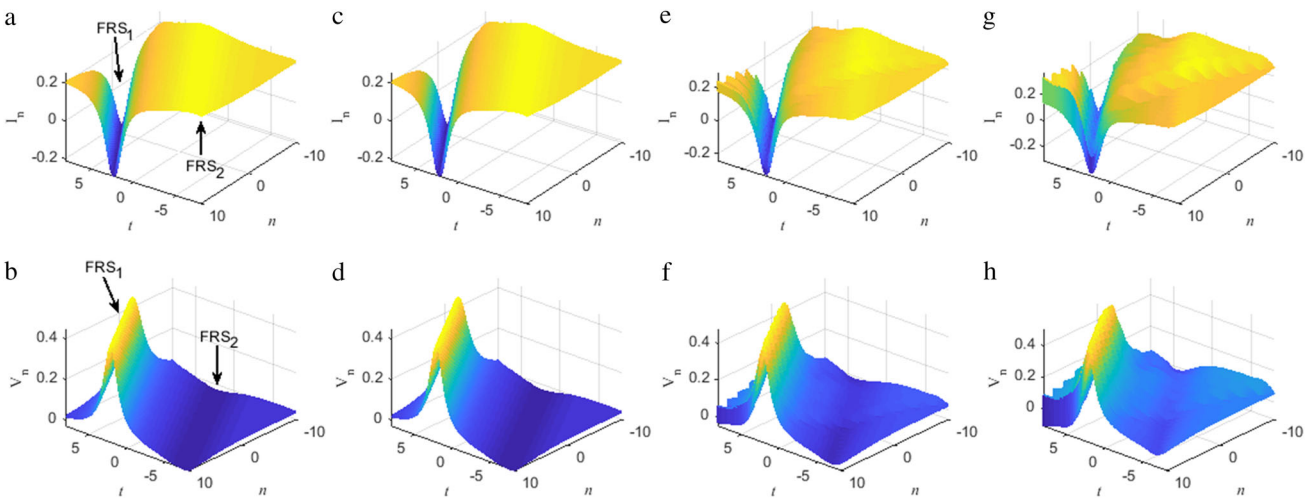

Figure 9. Numerical simulations of separatable second-order RS solutions $\tilde{I}_n$ and $\tilde{V}_n$ given by eq. (33) with $d_1 = 200$ (see figures 7b and 7d). (**a**)–(**b**) exact solution; (**c**)–(**d**) unperturbed situation; (**e**)–(**f**) perturbed by the initial 2% noise; (**g**)–(**h**) perturbed by the initial 5% noise.

the evolution without a noise agrees with the exact RS solutions in a relatively longer time interval and exhibits better stability.

Finally, we summarise a few wave features of discrete RS solutions I_n and V_n for eq. (1) in table 1. The first column in table 1 shows the order numbers of the solutions, while the second, third, fifth and sixth columns exhibit the powers of the polynomials involved in each pair of solutions. The fourth and last columns give the background levels of the solutions. From table 1, we can easily obtain the following information: provided the order N of the RS solutions is odd, the highest powers in the numerator polynomial of the solutions I_n and V_n are $2N(2N-1)-2$ and $2N(2N-1)$, respectively, while both the highest powers in the denominator polynomial are $2N(2N-1)$, and the background levels of the solutions I_n and V_n are zero and $-3/4$, respectively. On the other hand, supposing that the order N is even, the highest powers in the numerator polynomial of the solutions I_n and V_n are $2N(2N+1)$ and $2N(2N+1)-2$, respectively, while both the highest powers in the denominator polynomial are $2N(2N+1)$, and the back-

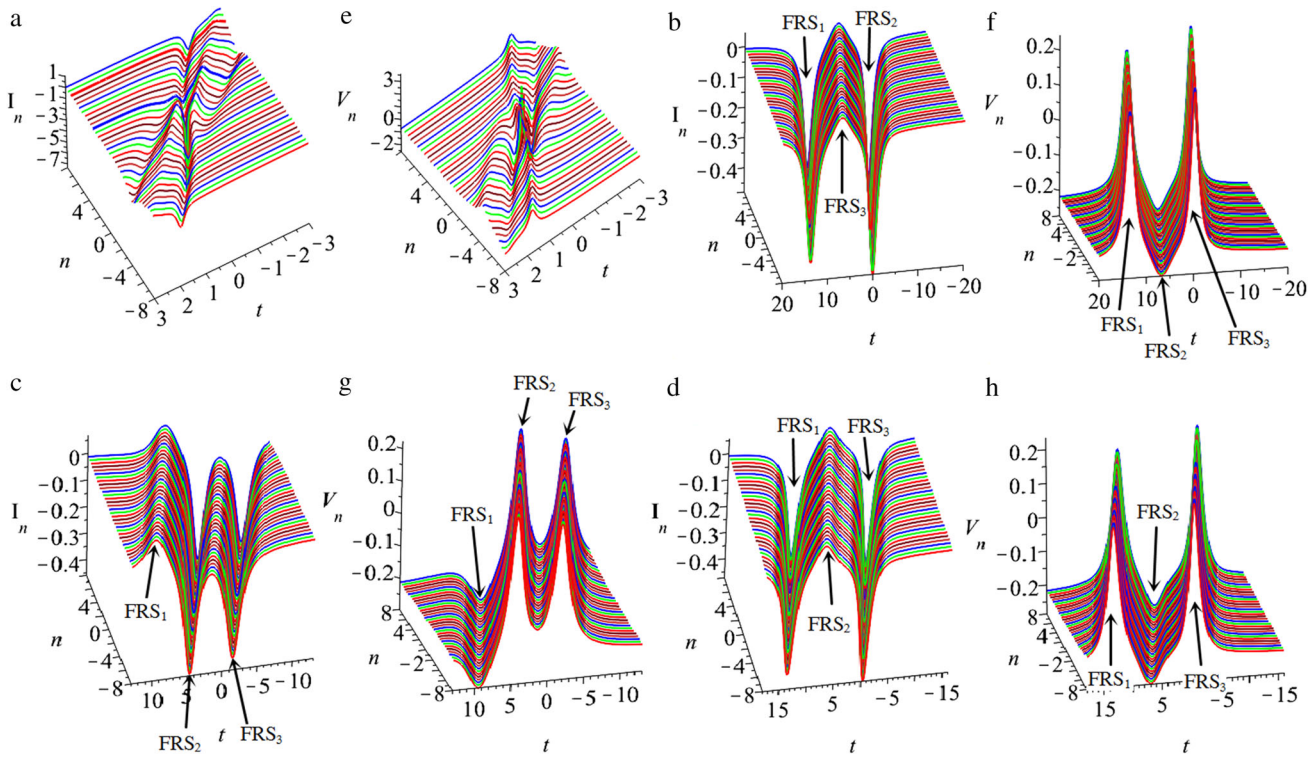

Figure 10. Evolution plots of third-order RS solutions $\tilde{I}_n$ and $\tilde{V}_n$ with different parameters (**a**), (**e**) $a = 3/4$, $\lambda_1 = 2$, $d_1 = d_2 = 0$; (**b**), (**f**) $a = 9/40$, $\lambda_1 = 5/4$, $d_1 = 100$, $d_2 = 0$; (**c**), (**g**) $a = 9/40$, $\lambda_1 = 5/4$, $d_1 = 0$, $d_2 = 800$; (**d**), (**h**) $a = 9/40$, $\lambda_1 = 5/4$, $d_1 = 100$, $d_2 = 400$. The phrases FRS_1, FRS_2 and FRS_3 stand for three parallel first-order RSs which are derived from the third-order RS solutions.

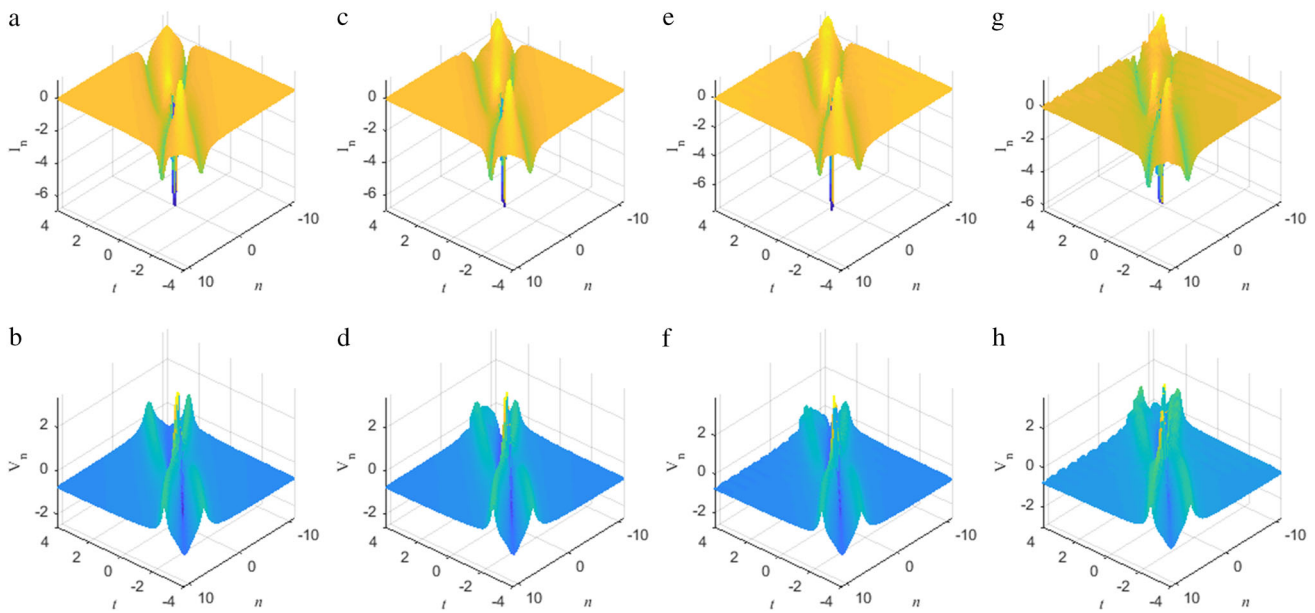

Figure 11. Numerical simulations of third-order interaction RS solutions $\tilde{I}_n$ and $\tilde{V}_n$ with same parameters as in figures 10a and 10e. (**a**), (**b**) exact solution; (**c**), (**d**) unperturbed situation; (**e**), (**f**) perturbed by the initial 2% noise; (**g**, **h**) perturbed by the initial 5% noise.

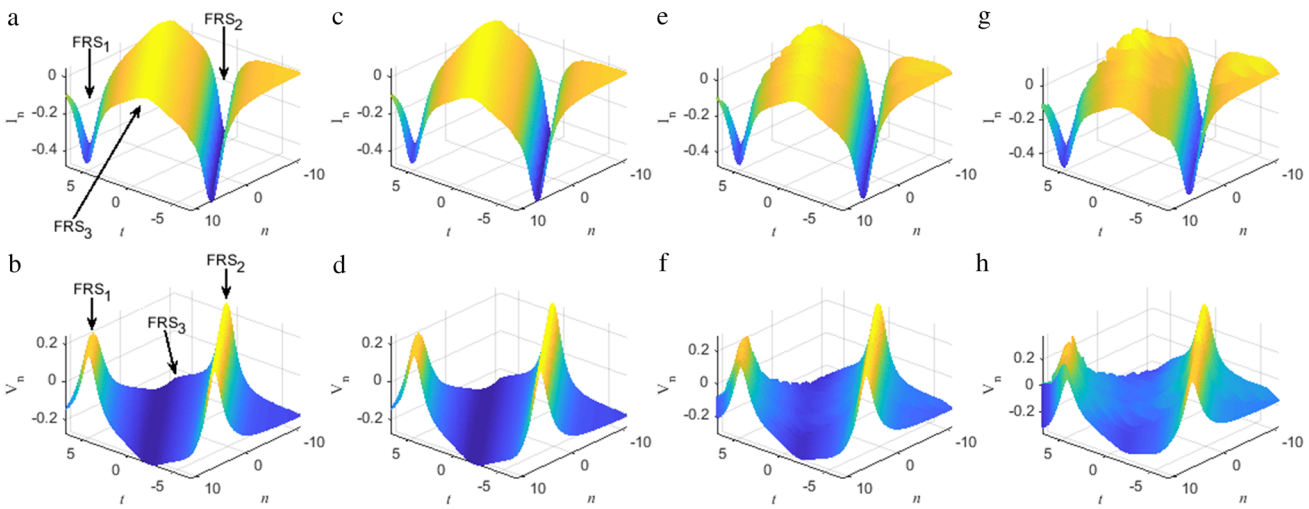

Figure 12. Numerical simulations of the separatable third-order RS solutions $\tilde{I}_n$ and $\tilde{V}_n$ with $d_1 = 100, d_2 = 0$ with the same parameters as in figures 10b and 10f. (**a**), (**b**) exact solution; (**c**), (**d**) unperturbed situation; (**e**), (**f**) perturbed by the initial 2% noise; (**g**), (**h**) perturbed by the initial 5% noise.

Table 1. Main mathematical features of rational solutions I_n and V_n of order N.

N	HPN of I_n	HPD of I_n	Background of I_n	HPN of V_n	HPD of V_n	Background of V_n
1	0	2	0	2	2	$-3/4$
2	6	6	$3/4$	4	6	0
3	10	12	0	12	12	$-3/4$
4	20	20	$3/4$	18	20	0
...	...	...	...	...	...	...
$2N-1$	$2N(2N-1)-2$	$2N(2N-1)$	0	$2N(2N-1)$	$2N(2N-1)$	$-3/4$
$2N$	$2N(2N+1)$	$2N(2N+1)$	$3/4$	$2N(2N+1)-2$	$2N(2N+1)$	0

Here, HPN and HPD stand for the highest powers in the numerator and denominator, respectively

ground levels of the solutions I_n and V_n are $3/4$ and zero, respectively.

5.2 *N-Soliton solutions on non-zero background of eq. (1) via N-fold DT*

In this section, we produce N-soliton solutions on non-zero constant seed background in terms of determinants for eq. (1) with $\sigma = 1$ by means of the discrete N-fold DT. In ref. [29], the N-fold DT of eq. (1) has been constructed and N-soliton solutions of eq. (1) on zero background has been given. N-Soliton solutions on non-zero constant seed background can also be similarly expressed, which are similar to the sech-type soliton solutions on zero background, but different from the standard sech-type soliton solutions. The interaction between this type of soliton solution and RS solution on the same non-zero constant seed background will be discussed in the next subsection through the discrete generalised $(2, N-2)$-fold DT. When $\sigma = -1$, the process is similar and will not be discussed due to its solutions possessing singularity. Substitution of $I_n = a$, $V_n = 0$ into (2) and (9) yields the following basic solution:

$$\varphi_n(\lambda) = \begin{pmatrix} C_1\tau_1^n e^{\rho_1 t} + C_2\tau_2^n e^{\rho_2 t} \\ C_1\dfrac{\lambda-\tau_1}{a}\tau_1^n e^{\rho_1 t} + C_2\dfrac{\lambda-\tau_2}{a}\tau_2^n e^{\rho_2 t} \end{pmatrix}, \tag{35}$$

with

$$\tau_1 = \frac{1}{2\lambda}(\lambda^2 + 1 + \sqrt{-(2a\lambda + \lambda^2 - 1)(2a\lambda - \lambda^2 + 1)}),$$

$$\tau_2 = \frac{1}{2\lambda}(\lambda^2 + 1 - \sqrt{-(2a\lambda + \lambda^2 - 1)(2a\lambda - \lambda^2 + 1)}),$$

$$\rho_1 = \frac{1}{2\lambda^2}(2a^2\lambda^2 + (\lambda^2 + 1)\sqrt{-(2a\lambda + \lambda^2 - 1)(2a\lambda - \lambda^2 + 1)}),$$

$$\rho_2 = \frac{1}{2\lambda^2}(2a^2\lambda^2 - (\lambda^2+1) \times\sqrt{-(2a\lambda+\lambda^2-1)(2a\lambda-\lambda^2+1)}),$$

where C_1, C_2 are arbitrary constants, $d_k (k = 1, 2, \ldots, N)$ are free real coefficients.

From Theorem 1, we can derive N-soliton solutions of eq. (1). When $N = 1$, the 1-fold explicit solutions of eq. (1) can be given as

$$\tilde{I}_n = \frac{a + b_n^{(0)}}{a_n^{(0)}}, \quad \tilde{V}_n = b_{n+1}^{(0)}, \tag{36}$$

if we choose $a = 3/4$, $C_1 = -C_2 = 1$, which can be rewritten as

$$\tilde{I}_n = \frac{\lambda_1(4-\lambda_1^2)(4\lambda_1^2-1)}{10\lambda_1^2(\lambda_1^2-1)\cosh\left[\frac{1}{2}(1+\frac{1}{\lambda_1^2})\eta_1 t + n\ln\frac{2\lambda_1^2+\eta_1+2}{2\lambda_1^2-\eta_1+2} + \frac{1}{2}\ln\frac{17\lambda_1^2-4\eta_1-8}{17\lambda_1^2+4\eta_1-8}\right] - 6\lambda_1^2(\lambda_1^2+1)},$$

$$\tilde{V}_n = \frac{(-\lambda_1^2+1)\{3\lambda_1\cosh\left[\frac{1}{2}(1+\frac{1}{\lambda_1^2})\eta_1 t + n\ln\frac{2\lambda_1^2+\eta_1+2}{2\lambda_1^2-\eta_1+2} + \frac{1}{2}\ln\frac{18\lambda_1^4+9\lambda_1^2\eta_1+86\lambda_1^2-16\eta_1-32}{18\lambda_1^4-9\lambda_1^2\eta_1+86\lambda_1^2+16\eta_1-32}\right] - 2\lambda_1^2+2\}}{4\lambda_1(\lambda_1+1)\sqrt{(\lambda_1-1)^2}\cosh\left[\frac{1}{2}(1+\frac{1}{\lambda_1^2})\eta_1 t + n\ln\frac{2\lambda_1^2+\eta_1+2}{2\lambda_1^2-\eta_1+2} + \frac{1}{2}\ln\frac{18\lambda_1^4+9\lambda_1^2\eta_1+86\lambda_1^2-16\eta_1-32}{18\lambda_1^4-9\lambda_1^2\eta_1+86\lambda_1^2+16\eta_1-32}\right] - 6\lambda_1^2},$$

(37)

where

$$\eta_1 = \sqrt{(\lambda_1^2-4)(4\lambda_1^2-1)}$$

and $\lambda_1 > 2$ is a real constant. It is worth noting that solutions (37) are sech-type soliton solutions with the same non-zero seed background as RS solutions in the previous subsection. With the same method and process, multisoliton solutions on the same non-zero seed background can also be obtained which are omitted here. The mixed interaction solutions on the non-zero seed background are discussed in the next subsection.

5.3 *Discrete generalised* $(2, N-2)$*-fold DT*

In the previous two subsections, we have used the discrete generalised $(1, N-1)$-fold DT with only one spectral parameter to derive the RS solutions of eq. (1), and we have used the discrete N-fold DT with N spectral parameters to derive the multisolutions of eq. (1) on non-zero background. Next, we shall use the discrete generalised $(2, N-2)$-fold DT with two spectral parameters to give some new interaction solutions of eq. (1). We only discuss two cases: $N = 2$ (i.e. the generalised $(2, 0)$-fold DT) and $N = 3$ (i.e. the generalised $(2, 1)$-fold DT).

5.3.1 *Mixed interaction of one US and one first-order RS via discrete generalised* $(2, 0)$*-fold DT.*

First, we set that $\lambda_1 = a + \sqrt{a^2+1}$ and $\lambda_2 \neq a + \sqrt{a^2+1}$ (e.g. $\lambda_2 = -6$). Then, we set the spectral parameter λ in eq. (35) as $\lambda = \lambda_1 + \varepsilon^2$, and expand the vector function φ_n in (35) as Taylor series around $\varepsilon = 0$ by choosing $C_1 = -C_2 = 1/\varepsilon$. Thus, $a_n^{(0)}$, $b_n^{(0)}$ and $b_n^{(1)}$ can be determined by the following system:

$$\begin{cases} T_n^{(0)}(\lambda_1)\varphi_n^{(0)}(\lambda_1) = 0, \\ T_n(\lambda_2)\varphi_n(\lambda_2) = 0, \end{cases} \tag{38}$$

with

$$a_n^{(0)} = \frac{\Delta a_n^{(0)}}{\Delta_2^{\varepsilon}}, \quad b_n^{(0)} = \frac{\Delta b_n^{(0)}}{\Delta_2^{\varepsilon}}, \quad b_n^{(1)} = \frac{\Delta b_n^{(1)}}{\Delta_2^{\varepsilon}}$$

and

$$\Delta_2^{\varepsilon} = \begin{vmatrix} \lambda_1\phi^{(0)} & \phi^{(0)} & \lambda_1\psi^{(0)} & \psi^{(0)} \\ \lambda_1\psi^{(0)} & \lambda_1^2\psi^{(0)} & -\lambda_1\phi^{(0)} & -\lambda_1^2\phi^{(0)} \\ \lambda_2\phi_{2,n} & \phi_{2,n} & \lambda_2\psi_{2,n} & \psi_{2,n} \\ \lambda_2\psi_{2,n} & \lambda_2^2\psi_{2,n} & -\lambda_2\phi_{2,n} & -\lambda_2^2\psi_{2,n} \end{vmatrix},$$

where $\Delta a_n^{(0)}$, $\Delta b_n^{(0)}$ and $\Delta b_n^{(1)}$ are given by the determinant Δ_2^{ε} replacing its second, fourth and third columns by the column vector $(-\lambda_1^2\phi^{(0)}, -\psi^{(0)}, -\lambda_2^2\phi_{2,n}, -\psi_{2,n})^T$, while $b_{n+1}^{(0)}$ is obtained from $b_n^{(0)}$ by replacing n with $n+1$.

Through the discrete generalised $(2, 0)$-fold DT, the explicit exact solutions of eq. (1) can be obtained as

$$\tilde{I}_n = \frac{a + b_n^{(1)}}{a_n^{(0)}}, \quad \tilde{V}_n = b_{n+1}^{(0)}. \tag{39}$$

Taking appropriate parameters, figure 13 shows the elastic interaction processes between one US and one first-order RS. Figure 13a shows the elastic interaction between one bright US and one dark first-order RS for $\tilde{I}_n$. Figure 13c shows the elastic interaction between one bright US and one bright first-order RS for $\tilde{V}_n$. Figure 13b displays the elastic interaction between one dark US and one bright first-order RS for $\tilde{I}_n$. Figure 13d

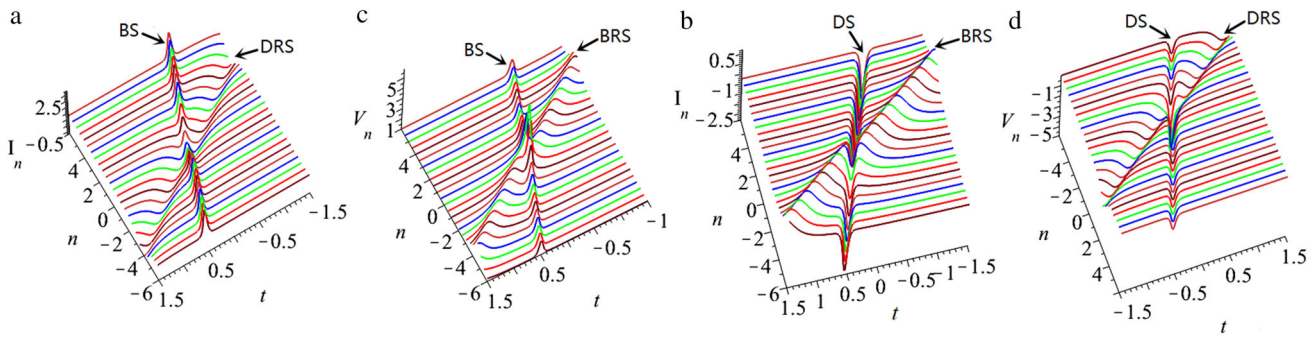

Figure 13. Mixed interaction of one-soliton and first-order RS solution with parameters (**a**), (**c**) $a = 3/4$, $\lambda_1 = 2$, $\lambda_2 = -6$; (**b**), (**d**) $a = -3/4$, $\lambda_1 = 1/2$, $\lambda_2 = -6$. The phrases DS, BS, DRS, BRS stand for dark soliton, bright soliton, dark first-order RS, bright first-order RS, respectively.

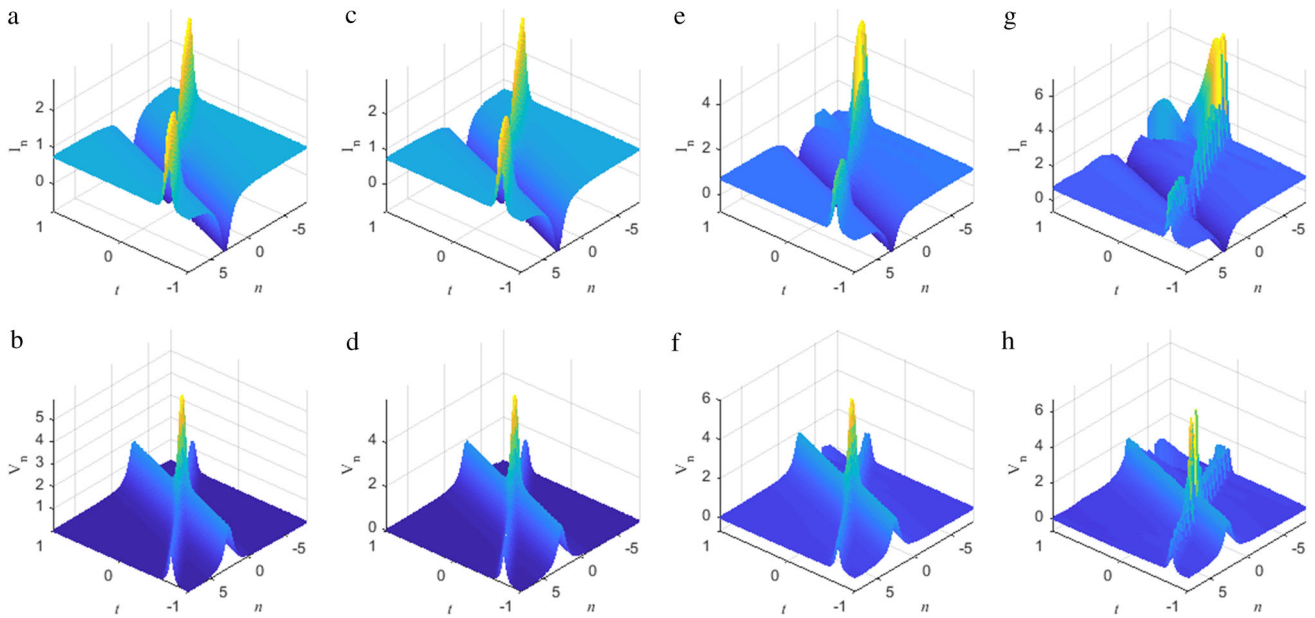

Figure 14. Numerical simulations of the interaction solutions $\tilde{I}_n$ and $\tilde{V}_n$ with the same parameters as in figures 13a and 13c. (**a**), (**b**) exact solutions; (**c**), (**d**) unperturbed situation; (**e**), (**f**) perturbed by the initial 2% noise; (**g**), (**h**) perturbed by the initial 5% noise.

exhibits the elastic interaction between one dark US and one dark first-order RS for $\tilde{V}_n$.

Figure 14 displays the numerical results by choosing parameters as in figures 13a and 13c. Obviously, the numerical results show that the 2% and 5% noises have no effect on the evolution of $\tilde{I}_n$ and $\tilde{V}_n$ in (39) except $\tilde{I}_n$ having a slight effect with 5%. These results show results nearly similar to one first-order RS (see figure 4).

5.3.2 *Mixed interaction of one US and second-order RS via discrete generalised* (2, 1)*-fold DT.* Similar to the previous process, setting $\lambda_1 = a + \sqrt{a^2+1}$ and $\lambda_2 \neq a + \sqrt{a^2+1}$ (e.g. $\lambda_2 = 6$), then we set the spectral parameter λ in eq. (35) as $\lambda = \lambda_1 + \varepsilon^2$, and expand the vector function φ_n in (35) as Taylor series around $\varepsilon = 0$ by choosing $C_1 = -C_2 = 1/\varepsilon$. Thus, $a_n^{(0)}$, $b_n^{(0)}$ and $b_n^{(2)}$ can be determined by the following system:

$$\begin{cases} T_n^{(0)}(\lambda_1)\varphi_n^{(0)}(\lambda_1) = 0, \\ T_n^{(0)}(\lambda_1)\varphi_n^{(1)}(\lambda_1) + T_n^{(1)}(\lambda_1)\varphi_n^{(0)}(\lambda_1) = 0, \\ T_n(\lambda_2)\varphi_n(\lambda_2) = 0, \end{cases} \tag{40}$$

with

$$a_n^{(0)} = \frac{\Delta a_n^{(0)}}{\Delta_3^{\varepsilon}}, \quad b_n^{(0)} = \frac{\Delta b_n^{(0)}}{\Delta_3^{\varepsilon}}, \quad b_n^{(2)} = \frac{\Delta b_n^{(2)}}{\Delta_3^{\varepsilon}}$$

and

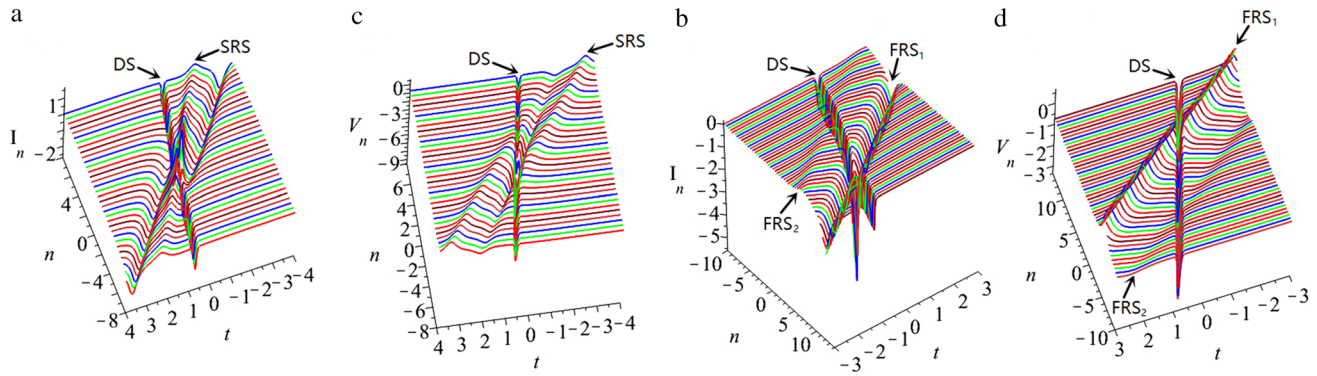

Figure 15. Mixed interaction solutions of one US and second-order RS with parameters (**a**), (**c**) $a = 3/4$, $\lambda_1 = 2$, $\lambda_2 = -6$, $d_1 = 0$; (**b**), (**d**) $a = 3/4$, $\lambda_1 = 2$, $\lambda_2 = -6$, $d_1 = 4$. The phrase SRS stands for second-order RS.

$$\Delta_3^{\varepsilon} = \begin{vmatrix} \lambda_1^2\phi^{(0)} & \lambda_1\phi^{(0)} & \phi^{(0)} & \lambda_1^2\psi^{(0)} & \lambda_1\psi^{(0)} & \psi^{(0)} \\ \Delta^{(2,1)} & \Delta^{(2,2)} & \Delta^{(2,3)} & \Delta^{(2,4)} & \Delta^{(2,5)} & \Delta^{(2,6)} \\ \lambda_1\psi^{(0)} & \lambda_1^2\psi^{(0)} & \lambda_1^3\psi^{(0)} & -\lambda_1\phi^{(0)} & -\lambda_1^2\phi^{(0)} & -\lambda_1^3\phi^{(0)} \\ \Delta^{(4,1)} & \Delta^{(4,2)} & \Delta^{(4,3)} & \Delta^{(4,4)} & \Delta^{(4,5)} & \Delta^{(4,6)} \\ \lambda_2^2\phi_{2,n} & \lambda_2\phi_{2,n} & \phi_{2,n} & \lambda_2^2\psi_{2,n} & \lambda_2\psi_{2,n} & \psi_{2,n} \\ \lambda_2\psi_{2,n} & \lambda_2^2\psi_{2,n} & \lambda_2^3\psi_{2,n} & -\lambda_2\phi_{2,n} & -\lambda_2^2\psi_{2,n} & -\lambda_2^3\psi_{2,n} \end{vmatrix},$$

$\Delta^{(2,1)} = \lambda_1^2\phi^{(1)} + 2\lambda_1\phi^{(0)}$, $\Delta^{(2,2)} = \lambda_1\phi^{(1)} + \phi^{(0)}$, $\Delta^{(2,3)} = \phi^{(1)}$, $\Delta^{(2,4)} = \lambda_1^2\psi^{(1)} + 2\lambda_1\psi^{(0)}$, $\Delta^{(2,5)} = \lambda_1\psi^{(1)} + \psi^{(0)}$, $\Delta^{(2,6)} = \psi^{(1)}$, $\Delta^{(4,1)} = \lambda_1\psi^{(1)} + \psi^{(0)}$, $\Delta^{(4,2)} = \lambda_1^2\psi^{(1)} + 2\lambda_1\psi^{(0)}$, $\Delta^{(4,3)} = \lambda_1^3\psi^{(1)} + 3\lambda_1^2\psi^{(0)}$, $\Delta^{(4,4)} = -\lambda_1\phi^{(1)} - \phi^{(0)}$, $\Delta^{(4,5)} = -\lambda_1^2\phi^{(1)} - 2\lambda_1\phi^{(0)}$, $\Delta^{(4,6)} = -\lambda_1^3\phi^{(1)} - 3\lambda_1^2\phi^{(0)}$, where $\Delta a_n^{(0)}$, $\Delta b_n^{(0)}$ and $\Delta b_n^{(2)}$ are given by the determinant Δ replacing its third, sixth and fourth columns by the column vector $(-\lambda_1^3\phi^{(0)}, -\lambda_1^3\phi^{(1)} - 3\lambda_1^2\phi^{(0)}, -\psi^{(0)}, -\psi^{(1)}, -\lambda_2^3\phi_{2,n}, -\psi_{2,n})^T$, while $b_{n+1}^{(0)}$ is obtained from $b_n^{(0)}$ by replacing n with $n+1$. Through discrete generalised (2, 1)-fold DT, an explicit exact solution of eq. (1) can be obtained as

$$\tilde{I}_n = \frac{a + b_n^{(2)}}{a_n^{(0)}}, \quad \tilde{V}_n = b_{n+1}^{(0)}. \tag{41}$$

Figure 15 shows the mixed interaction of one US and second-order RS for solutions (41) with (40). Figures 15a and 15c display the strong elastic interaction between one dark US and second-order RS. Figures 15b and 15d display the strong interaction of one dark US and two parallel first-order RSs which are derived from the second-order RS by choosing non-zero parameter d_1.

Here we need to explain that in §3, we know that the MI does not occur when $\sigma = 1$, the whole region is MS region, and US, RS and their mixed interaction solutions are all obtained in this stable region. In this section, we have performed the numerical analysis to check the stability of the derived solutions by adding 2% to 5% noises to these solutions. From these numerical simulation results, we can clearly see that these solutions remain stable evolutions for a longer period with 2% to 5% noises. That is to say, the stability of the numerical simulation of these solutions is consistent with the result through MI analysis. In addition, if we choose $\sigma = -1$, the derived solutions possess singularities so that we omit discussing them here.

It should be noted that the discrete generalised $(m, N-m)$-fold DT can give more abundant interaction structures of US and RS when $2 < m < N$. We shall not discuss these cases here.

6. Conclusions

In this paper, we have derived an integrable lattice hierarchy (6) from a discrete matrix spectral problem (2), and we have studied the second member eq. (1) with $\sigma = 1$ (i.e., the higher-order self-dual network equation) in this hierarchy, which may describe the propagation of electrical signals in a ladder-type nonlinear self-dual network. Starting from the non-zero seed solutions ($I_0 = a$, $V_0 = 0$), the MI of eq. (1) has been studied as shown in figure 2. Starting from Lax pairs (2) and (9), an infinite number of conservation laws (20)

have been explicitly given. We have constructed the discrete generalised $(m, N-m)$-fold DT for eq. (1), from which exact RS solutions, mixed interaction solutions of US and RS and numerical simulation results have been derived. In particular, one-, two- and three-RS solutions in terms of determinant for eq. (1) have been derived via the discrete generalised $(1, N-1)$-fold DT and relevant structures are shown graphically. Figure 3 exhibits the first-order RS structures of solutions I_n and V_n with $N = 1$, figures 4–6 show the dynamical evolutions of the first-order RS structures, figure 7 shows the second-order RS structures of solutions I_n and V_n with $N = 2$, figures 8 and 9 exhibit the dynamical evolutions of the second-order RS structures, figure 10 displays the third-order RS structures of solutions I_n and V_n with $N = 3$ and figures 11 and 12 display the dynamical evolutions of the second-order RS structures. Table 1 shows a few mathematical features of such RS solutions of eq. (1). By applying the discrete generalised $(2, N-2)$-fold DT, the mixed interaction solutions of US and RS have been obtained and the interaction structures are shown graphically. Figure 13 exhibits the interaction between one US and first-order RS with $N = 2$, numerical simulation results in figure 14 show the dynamical evolutions of such mixed interaction structures and figure 15 exhibits the interaction structures of one US and second-order RS with $N = 3$.

In theory, it is perfectly possible to expand eigenfunctions at more spectral parameters to get more new solutions of eq. (1) via the discrete generalised $(m, N-m)$-fold DT. However, in fact, the relevant calculations are very complex, and further investigation is needed. Finally, it is important to note that eq. (1) and new eq. (10) may provide the possibility for designing more complicated electrical circuits in LC circuits, and the results of this paper also provide a theoretical basis for seeking the propagation of stable electrical signals in electrical circuits. We hope that eq. (1) and its related results obtained in this paper might be helpful for understanding the propagation phenomena of electrical signals in practical application.

Acknowledgements

This work has been partially supported by National Natural Science Foundation of China under Grant Nos 12071042 and 61471406, Beijing Natural Science Foundation under Grant No. 1202006 and Qin Xin Talents Cultivation Program of Beijing Information Science and Technology University (QXTCP-B201704).

References

[1] A M Wazwaz, *Pramana – J. Phys.* **87**: 68 (2016)
[2] D W Zuo, *Appl. Math. Lett.* **79**, 182 (2018)
[3] H P Chai, B Tian, J Chai and Z Du, *Pramana – J. Phys.* **92**: 9 (2019)
[4] M Toda, *Theory of nonlinear lattices* (Springer, Berlin, 1989)
[5] W X Ma, *Physica A* **343**, 219 (2004)
[6] W X Ma and X X Xu, *J. Phys. A: Math. Gen.* **37**, 1323 (2004)
[7] D J Kaup, *Math. Comput. Simulat.* **69**, 322 (2005)
[8] M J Ablowitz and J F Ladik, *Stud. Appl. Math.* **57**, 1 (1977)
[9] M J Ablowitz and J F Ladik, *Stud. Appl. Math.* **55**, 213 (1976)
[10] X G Geng, *Acta Math. Sci.* **9**, 21 (1989)
[11] X Y Wen, *J. Phys. Soc. Jpn.* **81**, 114006 (2012)
[12] M Wadati, *Prog. Theor. Phys. Suppl.* **59**, 36 (1976)
[13] M Wadati and M Watanabe, *Prog. Theor. Phys.* **57**, 808 (1977)
[14] A Ankiewicz, N Akhmediev and J M Soto-Crespo, *Phys. Rev. E* **82**, 026602 (2010)
[15] A Ankiewicz, N Akhmediev and F Lederer, *Phys. Rev. E* **83**, 056602 (2011)
[16] R Hirota and K Suzuki, *J. Phys. Soc. Jan.* **28**, 1366 (1970)
[17] R Hirota, *J. Phys. Soc. Jpn.* **35**, 289 (1973)
[18] M J Ablowitz and J F Ladik, *J. Math. Phys.* **16**, 598 (1975)
[19] X G Geng, H H Dai and C W Cao, *J. Math. Phys.* **44**, 4573 (2003)
[20] X J Zhao, R Guo and H Q Hao, *Appl. Math. Lett.* **75**, 114 (2018)
[21] F J Yu and S Feng, *Math. Method Appl. Sci.* **40**, 5515 (2017)
[22] X Y Wen and D S Wang, *Wave Motion* **79**, 84 (2018)
[23] X Y Wen and Y Chen, *Pramana – J. Phys.* **91**: 23 (2018)
[24] H T Wang and X Y Wen, *Pramana – J. Phys.* **92**: 10 (2019)
[25] X Y Wen, Z Yan and B A Malomed, *Chaos* **26**, 123110 (2016)
[26] N Liu, X Y Wen and L Xu, *Adv. Differ. Equ.* **2018**, 289 (2018)
[27] X Y Wen and Z Y Yan, *J. Math. Phys.* **59**, 073511 (2018)
[28] X G Geng and H H Dai, *J. Math. Anal. Appl.* **327**, 829 (2007)
[29] C L Yuan, X Y Wen, H T Wang and Y Liu, *Chin. J. Phys.* **64**, 45 (2020)
[30] L C Zhao and L M Ling, *J. Opt. Soc. Am. B* **33**, 850 (2016)
[31] D Zhang and D Chen, *Chaos Solitons Fractals* **14**, 573 (2002)
[32] J K Yang, *Nonlinear waves in integrable and nonintegrable systems* (SIAM, Philadelphia, 2010)